

1 **Modeling Seasonal Effects of River Flow on Water Temperatures in an Agriculturally**
2 **Dominated California River**
3
4

5
6 **J. Eli Asarian¹, Crystal Robinson², [Laurel Genzoli³](#)**

7 ¹Riverbend Sciences, Eureka, CA, USA, ²Quartz Valley Indian Reservation, Fort Jones, CA,
8 USA, ³[Flathead Lake Biological Station and the University of Montana, Missoula, MT, USA](#)

9 Corresponding author: J. Eli Asarian (eli@riverbendsci.com)
10

11 **Key Points:**

- 12 • In this snowmelt and groundwater-influenced river, ~~cool~~ water temperatures ~~lasted~~
13 ~~longer~~ stayed cool later into summer in high-flow years than low-flow years
14 • Statistical water temperature model predictions became more accurate when the influence
15 of river flow was allowed to vary seasonally
16 • These accessible ~~methods~~ models can be ~~used~~ applied to ~~model any river~~ other rivers or
17 ~~stream~~ streams with daily, long-term flow and water temperature ~~measurements~~ records
18
19
20

21 **Abstract**

22 Low ~~summer river flows~~streamflows can increase vulnerability to warming, impacting coldwater
23 fish. Water managers need tools to quantify ~~the complex linkages~~these impacts and predict future
24 water temperatures. Contrary to most statistical models' assumptions, many seasonally changing
25 factors (e.g., water sources and solar radiation) cause relationships between flow and water
26 temperature, ~~yet statistical models often assume a constant relationship between these variables.~~
27 In California's snowmelt and groundwater-influenced Scott River where agricultural irrigation
28 consumes most summer river flow, flow variation had stronger effects on water temperature in
29 April–July than other months. Using 24 to vary throughout the year. Using 21 years of daily-air
30 temperature and flow data as predictors, we compared multiple statistical methods for
31 modeling modeled daily Scott River water temperatures, including in California's snowmelt-
32 driven Scott River where agricultural diversions consume most summer surface flows. We used
33 generalized additive models with non-linear interactions between flow and day-of-the-year to
34 test time-varying and nonlinear effects of flow on water temperatures. Models with that
35 represented seasonally varying flow effects performed better than those with intermediate
36 complexity outperformed simpler models assuming a constant relationship between
37 water temperature and flow. Cross-validation ~~root mean squared errors~~error of the selected
38 ~~models were ≤ 1 °C.~~model was ≤ 1.2 °C. Flow variation had stronger effects on water
39 temperatures in April–July than in other months. We applied the ~~models~~model to ~~several~~predict
40 effects of instream flow scenarios ~~currently being considered~~proposed by stakeholders and
41 regulatory agencies. Relative to historic conditions, the ~~most protective~~higher instream flow
42 scenario would reduce ~~average~~annual maximum temperature from 25.92 °C to 24.61 °C, reduce
43 ~~average annual degree-days exceedance~~exceedances of 22 °C (a cumulative thermal stress
44 metric) from ~~107106~~ to ~~5451~~degree-days, and delay ~~the onset of water temperatures greater than~~
45 >22 °C during some drought years. Withdrawal of river water after 1 June, including for
46 groundwater management purposes, could contribute to ~~Testing the same modeling approach at~~
47 nine additional exceedances of 22 °C. ~~sites showed similar accuracy and flow effects.~~ These
48 methods can be applied to ~~model any stream~~streams with long-term flow and water temperature
49 ~~measurements, with applications including scenario prediction and infilling~~records to fill data
50 gaps, identify periods of flow influence, and predict temperatures under flow management
51 scenarios.

52
53 **Plain Language Summary**

54 Warm water ~~threatens~~temperatures threaten culturally and economically important salmon in
55 Pacific Northwest rivers, ~~including our Scott River study area,~~ causing chronic stress ~~or even~~and
56 direct mortality. Climate change and agricultural water use have reduced summer river
57 ~~flow~~flows in recent decades, intensifying water scarcity. Years with deep mountain snowpack
58 and resulting high groundwater levels extend the high flow season and keep water temperatures
59 cool through the end of July, whereas in drought years the river warms sooner. We used ~~24~~21
60 years of river flow and air temperature data from the Scott River, California, to create computer
61 models that simulate water temperatures, ~~provide a tool for assessing the effects of water~~
62 management. Our models allow the effect of flow on water temperatures to vary by season (i.e.,
63 stronger cooling effects in spring and summer), improving accuracy of the simulated
64 temperatures. We used ~~these models~~the Scott River model to simulate water temperatures under

65 two alternative flow scenarios being considered in local water management plans. Our
66 simulations indicate that relative to current conditions, the higher flow scenario would
67 reduce lower the summer's hottest summers' highest temperatures. Diverting additional water
68 from the river after 1 June could increase and decrease the number of days with warm that river
69 temperatures that are detrimental to fish exceed a biological threshold. Testing the same modeling
70 approach at nine additional Klamath Basin sites showed similar accuracy and flow effects. Our
71 model is freely available for public use.

73 1 Introduction

74 Water temperature in rivers and streams affects everything from water chemistry drive physical,
75 chemical, and physics to inter-species interactions (Wenger et al., 2011), food webs (Power and
76 Dietrich, 2002), and whole community metabolism (Bernhardt et al., 2017). Effects on
77 individual species include development (Steel et al., 2012), thermal tolerances (Dahlke et al.,
78 2020), bioenergetics (Gibeau and Palen, 2020), and behavior (Sutton and Soto, 2012).

79 The net balance of surface and streambed heat fluxes determine stream temperatures. These
80 energy fluxes include shortwave radiation (primarily from the visible light spectrum), longwave
81 radiation (i.e., heat radiated from objects including clouds, land, and vegetation), latent heat (i.e.,
82 evaporation), sensible heat (i.e., convection of heat from air to water), conduction of heat
83 between the water and stream bed, and advection (i.e., movement of water) (Caissie, 2006;
84 Moore et al., 2005a; Webb et al., 2008; Dugdale et al., 2017). Humans affect stream
85 temperatures through water diversions (Bartholow, 1991; Dymond J., biological processes
86 (Ouellet et al., 2020), 1984; Folegot et al., 2018; Gibeau and Palen, 2020; Meier et al. 2003, Null
87 et al.; 2017), discharge of industrial wastewater and sewage (Erickson and Stefan, 2000),
88 reservoir impoundments (Webb and Walling, 1993; Chandesris et al., 2019), removal or
89 enhancement of riparian vegetation (Johnson, 2004; Moore et al. 2005a, Wondzell et al., 2019),
90 and alteration of channel and floodplain morphology (Gu and Li, 2002) including urbanization
91 (Tan and Cherkauer, 2013). Stream temperatures have warmed in recent decades in response to
92 rising air temperatures resulting from anthropogenic greenhouse gas emissions, a trend that is
93 expected to continue (Isaak et al., 2017, 2018; Liu et al., 2020; Wanders et al., 2019).

94 determine species River flow rates (i.e., discharge) can affect stream temperatures. Higher flows
95 increase a stream's ability to store heat, reducing the temperature increase resulting from an
96 equivalent amount of solar radiation (Brown, 1969; Meier et al., 2003; Sinokrot and Gulliver,
97 2000). Higher flow rates reduce daily temperature maximums and ranges (Folegot et al., 2018).
98 Summer, with alterations to natural temperature regimes causing deleterious effects to native
99 species (Wenger et al., 2011). Stream temperatures are widely altered by human activities (Webb
100 et al., 2008). Maintaining ecological integrity is a major stream temperature management goal,
101 yet models used to predict stream temperature response to management interventions either lack
102 predictive power or are time-consuming to develop.

103 River flow rates (i.e., discharge) are a key driver of stream temperatures through multiple
104 mechanisms. While stream temperatures are determined by surface and streambed energy fluxes
105 and advected heat (Caissie, 2006; Moore et al., 2005), flows mediate these effects. Higher flows
106 generally increase water volume and thus a stream's capacity to store heat, reducing daily
107 temperature fluctuations (Brown, 1969; Folegot et al., 2018; Meier et al., 2003; Sinokrot &

108 Gulliver, 2000). Higher flows speed downstream transit of water, reducing the time that a parcel
109 of water is exposed to ambient heating at a given location and increasing the influence of
110 upstream conditions (Bartholow, 1991; Dymond J., 1984; Folegot et al., typically negatively
111 correlated with flow (Arora et al., 2016; Isaak et al., 2017; Luce et al., 2014; Mayer, 2012;
112 McGrath et al., 2017; Moore, et al. 2005b; Neumann et al., 2003; Webb et al., 2003), with flow
113 affecting daily maximum temperatures more strongly than daily mean temperatures (2018).
114 Channel geometry, including width/depth ratio, influences these effects (Dugdale et al., 2017).
115 (Asarian et al., 2020; Gu et al., 1998; Gu and Li, 2002). Stream temperature model fit often
116 increases when flow is included as a predictor (Hilderbrand et al., 2014; Piotrowski and
117 Napiorkowski, 2019; Rahmani et al., 2020; Sohrabi et al., 2017; van Vliet et al., 2011; Webb et
118 al., 2003), although not always (Benyahya et al., 2008; Toffolon and Piccolroaz, 2015). Cooling
119 effects of high flows are due to faster downstream transport of cold water (Bartholow, 1991;
120 Dymond J., 1984; Folegot et al., 2018), greater depth and thermal mass which is more resistant
121 to heating (Gu and Li, 2002; Meier et al., 2003; Sinokrot and Gulliver, 2000), and greater
122 accretion of cool groundwater (Kelleher et al., 2012; Mayer, 2012; Isaak et al., 2017).

123 The relationship between water temperature and flow varies seasonally. The source and flow
124 paths of river water vary seasonally according to through time. Seasonal changes in precipitation
125 form phase (i.e., snow and rain) (Siegel and Volk, 2019), groundwater dynamics of hillslope
126 (Hahn et al., 2019) and alluvial (Foglia et al., 2013) aquifers, and irrigation management (i.e.,)
127 affect water temperatures (Yan et al., 2021). The geographical source of water can shift
128 seasonally, and can include tributaries, point sources, hillslopes, and alluvial aquifers, with each
129 source having different temperatures and heating or cooling trajectories while en route to stream
130 channels (Dugdale et al., 2017; Steel et al., 2017). Groundwater-surface water interactions and
131 hyporheic exchange also affect temperatures (Hannah et al., 2009; Kurylyk et al., 2015). Water
132 management, including reservoir releases, water withdrawals, and subsequent return flows back
133 to the river via surface or groundwater (Tolley) irrigation runoff can further alter temperature
134 dynamics (Alger et al., 2021; Chandesris et al., 2019). Flow effects on water temperature are also
135 seasonally further mediated by variables that affect the amount of seasonal changes to solar
136 radiation striking received by the water, including stream. Day length, and solar angle, which
137 affect topographic and riparian shading, remain consistent among years (Piotrowski and
138 Napiorkowski, 2019; Yard et al., 2005), cloud cover (Dugdale et al., 2017), wildfire smoke
139 (Asarian et al., 2005). Other mediators of solar radiation including 2020; David et al., 2018), and
140 leaf out and leaf fall of deciduous riparian vegetation, cloud cover (Dugdale et al., 2017), water
141 vapor, dust (Theurer et al., 1984), wildfire smoke (Asarian et al., 2020; David et al., (Dugdale et
142 al., 2018). Some of these variables (2018) and other aerosols follow exactly the same seasonal
143 trajectory each year while others fluctuate among years. seasonal trajectories that vary among
144 years. Despite time-varying changes in how flow dynamics influence stream temperature, many
145 stream temperature models do not account for these seasonal variations in the relationship
146 between flow and stream temperatures.

147 Given stream temperature's importance and vulnerability to human alterations of river flow,
148 water managers need predictive tools to predict stream temperature models are often grouped
149 into two categories: process-based changes associated with climate change and statistical
150 (Caissie, 2006) flow management (Gibeau & Palen, 2020; Null et al., 2017). While process-
151 based (i.e., deterministic) models simulate stream energy budgets using physically
152 based equations representing energy fluxes such as shortwave radiation, longwave radiation,

153 latent heat, sensible heat, conduction and advection can have high predictive accuracy, their use is
154 limited by extensive data input requirements (Brown, 1969; Caissie, 2006; Dugdale et al., 2017).
155 Statistical models that use empirical relationships between stream temperature and predictor
156 variables, and typically environmental drivers require many fewer input variables as data inputs
157 than process-based models do, so are often much simpler to develop (Benyahya et al., 2007;
158 Caissie, 2006; Gallie et al., 2015; Ouellet et al., 2020; Piotrowski and Napiorkowski, 2019).
159 Mohseni et al.'s (1998) non-linear regression of stream temperature and air temperature has been
160 widely replicated (Arismendi et al., 2014; Jones et al., 2016) and adapted (Piotrowski and
161 Napiorkowski, 2019; Santiago et al., 2017; Segura et al., 2015; van Vliet et al., 2011). Recent
162 advances in statistical models of stream temperature include spatial stream network models
163 (FitzGerald et al., 2021; Isaak et al., 2017), generalized additive models (GAM) (Arora et al.,
164 2016; Jackson et al., 2018; Laanaya et al., 2017; Siegel and Volk, 2019; Yang and Moyer, 2020),
165 Least Absolute Shrinkage and Selection Operator regression (St Hilaire et al., 2018), functional
166 data analysis (Boudreault et al., 2019), and machine learning (Rahmani et al., 2020; Zhu et al.,
167 2018, 2020). Daily stream temperatures are highly correlated with adjacent days' temperatures.
168 For measurements such as daily stream temperature that are not independent, it is best easier to
169 use a model that explicitly includes the correlation structure (Steel et al., 2013). For example,
170 some stream temperature models include a first order (AR-1) (Benyahya, 2007b; David et al.,
171 2018; Letcher et al., 2016; Jackson et al., 2018; Sohrabi et al., 2017), second-order, periodic
172 (implement, but for scenario prediction they are generally not considered as reliable as process-
173 based models (Arismendi et al., 2014; Benyahya et al., 2007a, 2007b, 2008), or moving average
174 autoregressive error structures (Yang and Moyer, 2020).

175 Process-based models account for the seasonal effects of flow by explicitly modeling energy
176 fluxes, but it is infeasible to include all these individual fluxes in statistical model; Caissie,
177 2006). However, statistical models can represent the implicit aggregation of these fluxes by
178 allowing the coefficients of hydroclimatic predictors to vary seasonally. One approach is to
179 divide the year into multiple seasons and develop separate models for each (Mohseni et al., 1998,
180 Sohrabi et al., 2017), but this may create abrupt changes at seasonal transitions. Recent
181 approaches that allow smooth variation across seasons are time-varying coefficient models (Li et
182 al., 2014), and GAMs that interact day-of-the-year with predictor variables (Jackson et al., 2018;
183 Siegel and Volk, 2019; Yang and Moyer, 2020) modeling methods have evolved, improving
184 prediction accuracy and temporal resolution (i.e., daily) (Ouellet et al., 2020; Piotrowski &
185 Napiorkowski, 2019). Year-round daily temperature models are especially valuable because they
186 match the time scales used in detailed biological studies and water quality regulations (Imholt et
187 al., 2010; Railsback et al., 2015; USEPA, 2003).

188 Statistical stream temperature models have long relied on air temperature as the primary
189 predictor (Mohseni et al., 1998), but year-round daily models should incorporate additional
190 mechanisms to improve accuracy and reflect physical processes (Letcher et al., 2016). Statistical
191 stream temperature models use air temperature to represent net radiative flux (Caissie 2006).
192 Time lags between air temperatures and water temperature reflect heat exchange processes
193 (Koch and Grünwald, 2010; Soto, 2016; Webb et al., 2003), while temporal autocorrelation
194 acknowledges that stream temperature on a given day is in part a result of stream temperature the
195 previous day (Benyahya et al., 2007a, 2007b, 2008; Yang & Moyer, 2020). Inclusion of flow can
196 improve model accuracy (Piotrowski & Napiorkowski, 2019; Santiago et al., 2017; Sohrabi et
197 al., 2017; van Vliet et al., 2011; Webb et al., 2011). To test the hypothesis that statistical models with
198 seasonally varying effects of river flow would perform better than models with a constant

199 relationship between stream temperature and flow, we modeled daily stream temperatures in the
200 Scott River of Northern California where low flows and high temperatures are limiting factors
201 for culturally and economically important coldwater fish. We compared multiple statistical
202 approaches that: 1) include all days in a single model rather than dividing the year, 2) use
203 interactions to allow the influence of predictors to vary smoothly by day of the year, 3) allow
204 non-linear relationships, 4) have error structures that include temporal autocorrelation, and 5) are
205 all implemented within the R software environment with simple, publicly accessible code. After
206 model selection and validation which confirmed our hypothesis, we applied our final model to
207 predict daily stream temperatures under flow scenarios being considered by local water
208 managers. Results indicated that stream temperatures under these flow scenarios would be more
209 favorable for coldwater fish than the historic flow scenario. Our accessible modeling approach
210 could be widely replicated in other geographic areas to provide accurate stream temperature
211 predictions to inform river management. Paired with air temperatures from a nearby weather
212 station, our methods can be applied in any river or stream with long term measurements of flow
213 and stream temperature. Other potential applications include imputing missing measurements for
214 analyses that require continuous temperature time series.

215 2003). The relationship between air and stream temperatures is nonlinear and differs among
216 seasons (Arismendi et al., 2014; Caissie et al., 2001; Mohseni et al., 1998). Including time-
217 varying effects could improve the predictive accuracy of stream temperature models across
218 variable conditions.

219 Several methods allow seasonal variation in the relationship between environmental covariates
220 and stream temperatures. These methods not only improve model accuracy but also identify the
221 times when effects are strongest. While time-varying covariate effects can be represented using
222 separate models for each season (Mohseni et al., 1998; Sohrabi et al., 2017), this may cause
223 unnatural, abrupt changes at seasonal transitions. Time-varying coefficients, including those used
224 in generalized additive models (GAMs) (Pedersen et al., 2019; Wood, 2017) use continuous
225 functions that avoid these abrupt changes (Li et al., 2014; Jackson et al., 2018; Siegel & Volk,
226 2019). While GAMs have been used in daily stream temperature modeling for single-site
227 prediction (Boudreault et al., 2019; Coleman et al., 2021; Glover et al., 2020; Laanaya et al.,
228 2017), spatiotemporal prediction (Jackson et al., 2018; Siegel & Volk, 2019), identifying
229 extreme events (Georges et al., 2021), and trend assessment (Yang & Moyer, 2020), few studies
230 have used GAMs to model seasonally varying flow effects or identify when stream temperatures
231 are most affected by flow variation (Glover et al., 2020; Yang & Moyer, 2020). With flexible
232 model structures and easy implementation, GAMs could be a powerful tool for predicting stream
233 temperatures under flow management scenarios, but to our knowledge these models have not
234 been previously used for this purpose.

235 Our objectives were to predict mean and maximum daily stream temperatures under management
236 flow scenarios and new environmental conditions, and to identify periods when flow has the
237 strongest influence on stream temperatures. We compared 11 GAM structures using flow, air
238 temperature, and day of year as covariates that incorporated combinations of linear, nonlinear,
239 and seasonally-varying effects. Our model selection and validation procedures included
240 extrapolation tests evaluating predicted stream temperatures with flows and air temperatures
241 outside the calibration range, designed to favor models that had enough complexity to represent
242 the key patterns in the data, but not so complex that they overfit the data. We applied the top
243 model to proposed management flow scenarios and extreme flow and air temperature conditions.

244 The models are intended to be used as a tool to inform water management, making the relatively
245 simple model structure and coding of GAMs our choice of modeling technique. We focused our
246 analyses on the Scott River of Northern California, where low flows and high temperatures are
247 limiting factors for coldwater fish and water managers are considering implementing regulations
248 to protect instream flows. To demonstrate wider applicability, we evaluated similar models in
249 nine additional sites in the Klamath River Basin.

251 2 Study Area

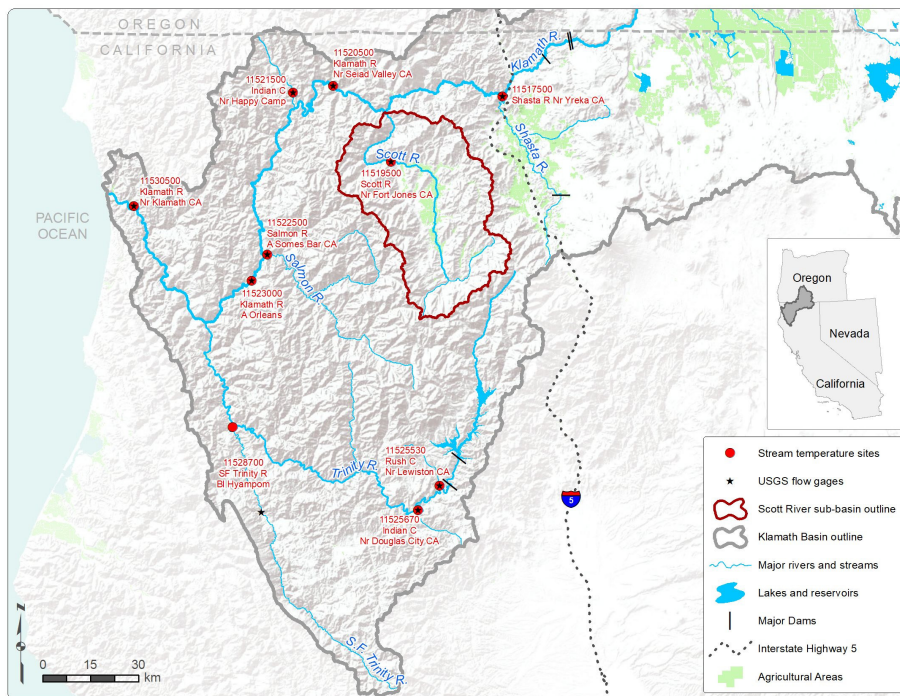
252 The Scott River is a tributary of the Klamath River in Siskiyou County, California, USA (Figure
253 1). Our study area is the lower Klamath River Basin, California, USA, focusing on one large
254 tributary—the Scott River (Figure 1). The Scott River study site is located at the outlet of Scott
255 Valley, with a drainage area of 1,714 km². The other nine sites are near USGS gaging stations
256 with drainage areas ranging from 58 km² to 31,300 km² (Figure 1, Table S1). The climate is
257 Mediterranean with precipitation occurring primarily in winter and spring as rain at low
258 elevations and snow at higher elevations. The mountainous headwaters are primarily National
259 Forest, with elevations exceeding 2500m (Foglia (VanderKooi et al., 2013)2011). The human
260 population lives primarily on private land in the alluvial along watercourses including Scott
261 Valley, where irrigated agriculture is the dominant/ dominates land use, utilizing groundwater and
262 surface water (Foglia et al., 2018). Other land uses include timber harvest and mining. There are
263 many water diversions but The Scott River has no major dams or reservoirs-, but there are large
264 dams on the Klamath River and two tributaries (Shasta and Trinity rivers), influencing some
265 study sites.

266 The Scott Valley aquifer fills during the high flows of winter rainstorms and spring snowmelt-
267 driven runoff. As runoff recedes through the summer, most surface water is diverted for
268 irrigation and river water at the Scott Valley outlet becomes increasingly composed of
269 groundwater from valley alluvium. Minimum flows occur in early September before rising due
270 to fall rains (Figure 22b). In late summer of drought years, portions of the Scott River have no
271 surface flow (Tolley et al., 2019). Summer and fall river flows have declined in recent decades
272 (Kim and Jain, 2010; Asarian and Walker, 2016) due to a combination of climate change (Drake
273 et al., 2000) and increased withdrawal of groundwater for irrigation/ withdrawals, especially since
274 1977 (Van Kirk and Naman, 2008). Climate change is expected to further reduce summer flows
275 by decreasing snowpack and increasing irrigation demand (Persad et al., 2020). There are
276 ongoing efforts to model interactions between groundwater and surface water (Foglia et al.,
277 2013, 2018; Tolley et al., 2019). Pursuant to California's Sustainable Groundwater Management
278 Act (SGMA), Siskiyou County is developing a groundwater sustainability plan for the valley.

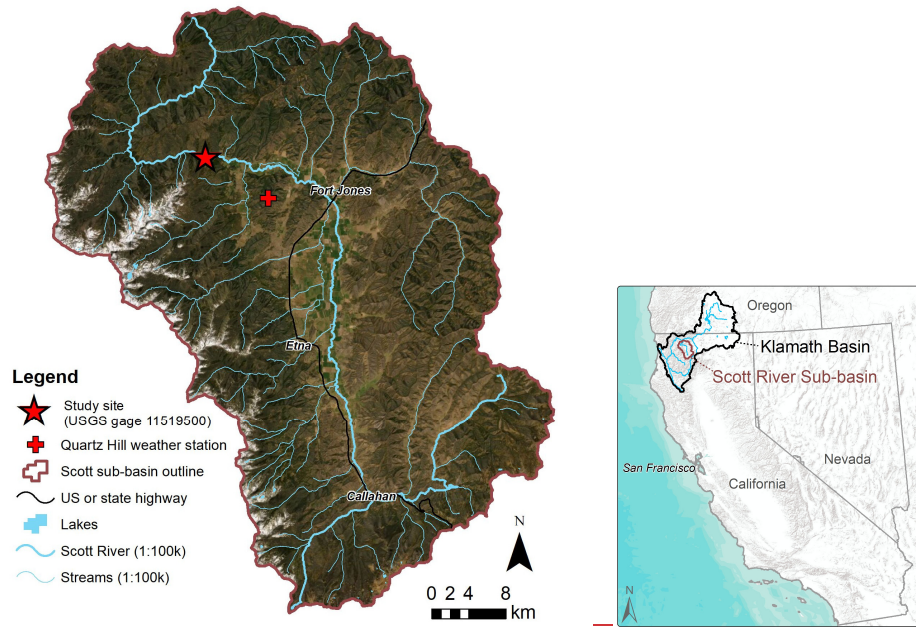
279 Management flows have been proposed for the Scott River has the Klamath Basin's largest
280 population of to protect Endangered Species Act-listed coho salmon (*Oncorhynchus kisutch*)
281 population, despite currently impaired habitat (NMFS, and other coldwater salmonid fishes,
282 2014). High water temperatures are stressful to coho salmon, chinook salmon (*Oncorhynchus*
283 *tshawytscha*) and steelhead (*Oncorhynchus mykiss*) (NCRWQCB, 2005). These fishes'
284 importance to local Native American tribes has led to contention over water management.
285 Government agencies, tribes, River water temperatures in May–July are much cooler in high-flow
286 years than low-flow years (Figure 2), and local organizations have studied Scott River stream
287 temperatures for several decades (Asarian et al., 2020; KNF, 2010; Quigley et al., 2001; QVIR,

288 2016). The river is water extraction has contributed to the Scott River being listed as impaired for
 289 water temperature under the Clean Water Act (NCRWQCB, 2005). The U.S. Forest Service has
 290 a first-priority Schedule D water right for Scott River instream flow that varies by month and
 291 California's North Coast Regional Water Quality Control Board developed Total Maximum
 292 Daily Loads (TMDLs) for water temperature day from 30–200 ft³/s (0.85–5.67 m³/s) (Superior
 293 Court of Siskiyou County, 1980) (Figure 3b), but does not exercise its legal authority to curtail
 294 lower-priority water uses when flows drop below these levels. The California Department of Fish
 295 and sediment (NCRWQCB, 2005)–Wildlife (CDFW) proposed interim Scott River instream
 296 flow targets that vary by month and day from 62–362 ft³/s (10.3–1.75 m³/s) (CDFW, 2017)
 297 (Figure 3b), but these have no legal force.

298 Our

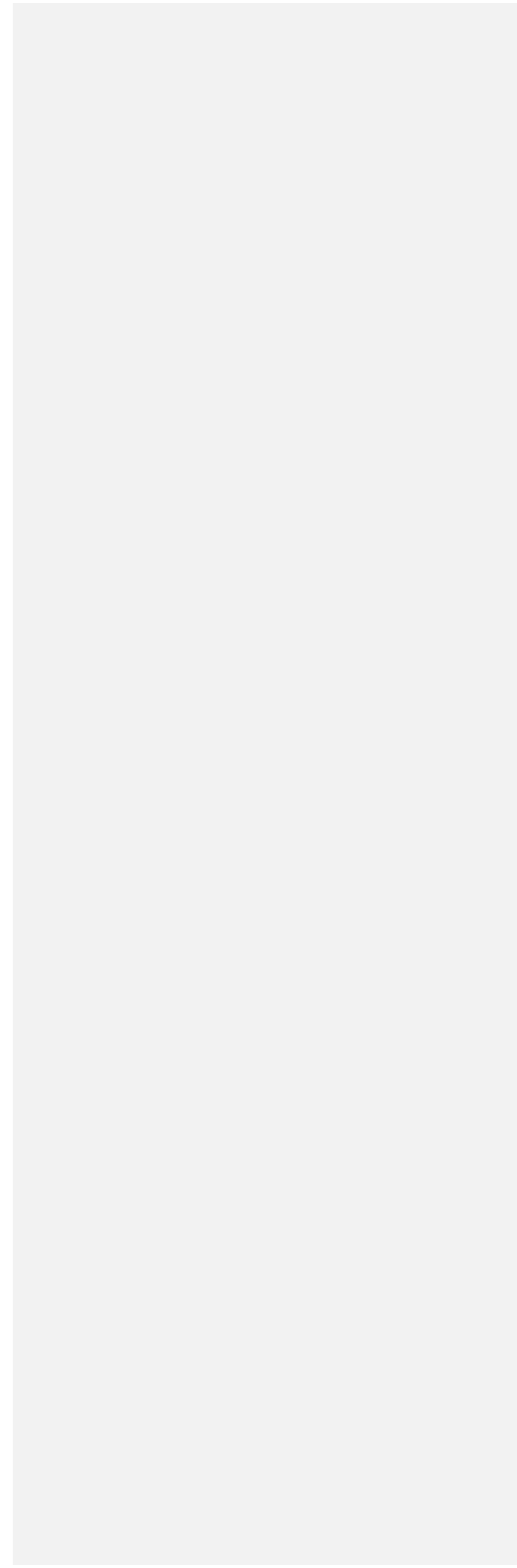
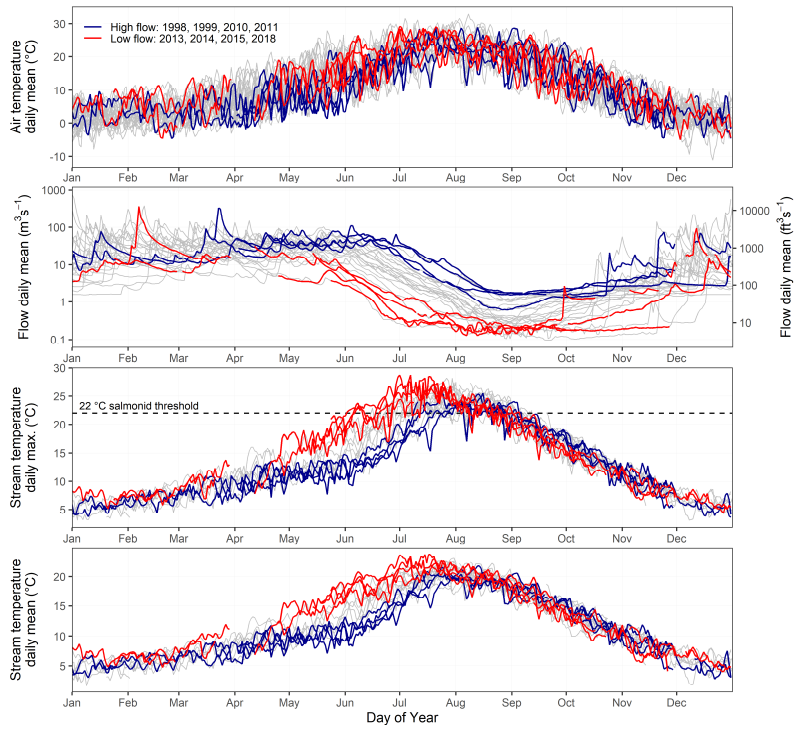


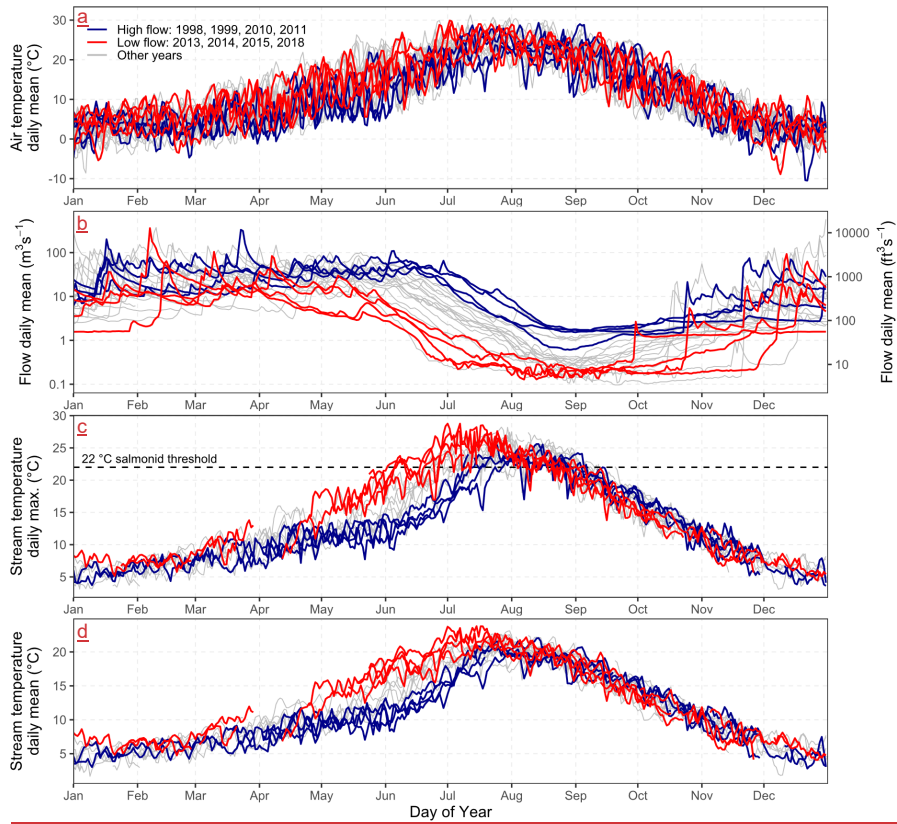
301 Figure 1. Klamath Basin study site is located at the outlet of Scott Valley, sites with a drainage
 302 area of 1,714 km² (Figure 1). Despite simulated total valley wide streamflow depletion (i.e.,
 303 decreased streamflow due to groundwater pumping) of approximately 150,000 m³ d⁻¹ (60 ft³/sec)
 304 in August (Foglia et al., 2013), the 10 kilometers of river directly upstream of our study site are
 305 primarily a gaining reach, receiving groundwater from the alluvial aquifer (Tolley et al., 2019).
 306



307
308 **Figure 1.** Maps of study site and weather station within the Scott River Watershed, the Klamath
309 Basin, and California, outlined in red. Source map credits: Esri, Earthstar Geographics, NOAA,
310 and USGS.

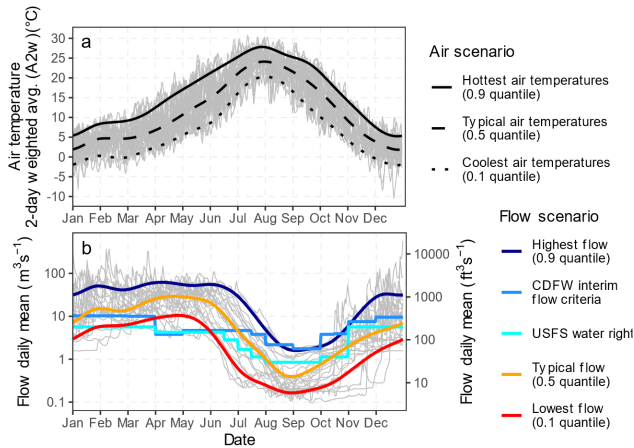
311





313
314 **Figure 2.** Time series of (a) daily mean air temperature, (b) daily mean flow, (c) daily maximum
315 stream temperature ($DM_{xST_{max}}$), and (d) daily mean stream temperature ($DMST$) for the years
316 $1998_{T_{mean}}$ at Scott River from 1998–2020.

317
318



319
 320 **Figure 3.** Inputs to Scott River “quantile air temperature” scenarios representing 15
 321 combinations of (a) three air temperature inputs and (b) five flow inputs that vary by day.
 322 Observed values for 1998–2020. Colored lines are shown as gray lines are days in four example high-
 323 flow (red) and low-flow years (blue). Gray lines are other years.

324

325 **3 Methods**

326 At each of the 10 sites, we developed GAMs to predict daily mean stream temperature (T_{mean})
 327 and daily maximum stream temperature (T_{max}) using flow, air temperature, and day of year as
 328 covariates. We compared models across a range of complexity, including those with seasonally
 329 varying flow effects, to models with a constant relationship between stream temperature and
 330 flow. We selected a final model based on the best overall performance averaged across the 10
 331 sites. We then applied that model to flow management scenarios at one site– the Scott River.

332 **3.1 Data sources and data preparation**

333 **3.1.1 Water temperature and river flow**

334 Since 2007, we obtained water temperature data from six sources (Table S1). For the Scott River
 335 site, we used Quartz Valley Indian Reservation (QVIR) Environmental Department has been
 336 using YSI (Yellow Springs, Ohio) 6600 multi-parameter datasondes to monitor Scott River water
 337 temperatures at the U.S. Geological Survey (USGS) gage 11519500 near the outlet of Scott
 338 Valley (QVIR, 2016; Asarian et al., 2020) (Figure 1). Temperature measurements are recorded
 339 every 30 minutes with a reported accuracy of ± 0.15 °C. We combined QVIR’s dataset with
 340 additional temperature data collected at the same site data, supplemented by the U.S. Forest
 341 Service (USFS) in the years 1995–1998, 2003–2005, 2010–2016, and 2019 (KNF, 2010), 2011
 342 and U.S. Bureau of Reclamation (USBR) for the years 1998–2000 (Smith et al., 2018) data. For
 343 the nine other sites, we used data from the U.S. Fish and Wildlife Service (USFWS) (Manhard et
 344 al., 2018; Romberger and Gwozdz, 2018), USFS (KNF, 2010, 2011), USBR, U.S. Geological
 345 Survey (USGS), and California Department of Water Resources (CDWR). Following

346 compilation, we reviewed the data and removed any suspicious values (e.g., when there were
 347 calibration issues or probes appear to have been exposed to air). We then calculated daily mean
 348 stream temperature (DMST) T_{mean} and daily maximum stream temperature (DMxST) T_{max} . For
 349 days when data were available from multiple entities, we averaged values (Text S1). Data
 350 availability ranged from 3540–5684 days and 16–21 years per site. We paired daily temperatures
 351 at each site with daily average streamflow data from nearby USGS gages (Figure 1, Table S1).
 352 Daily average streamflow for gage 11519500 were downloaded from the USGS National Water
 353 Information System.

354 3.1.2 Air temperature

355 We retrieved daily mean air temperature data from USFS’ Quartz Hill weather station located
 356 approximately 8 km southeast of the flow gage (Figure 1) are available as Global Historical
 357 Climatology Network—Daily station USR0000CQUA (Menne et al., 2012a, 2012b). We
 358 excluded all dates with a quality flag. For days lacking Quartz Hill measurements (0.5% of days
 359 with measured stream temperatures and 3.8% of the all days 1995–2020), we infilled missing
 360 values by linear regression with nearby weather stations or the temperatures for each site from the
 361 4-km resolution gridded PRISM dataset (Daly et al., 2008) (Text S2).

362). Because stream temperatures are correlated with air temperatures, temperature at multiple time
 363 scales. The optimal number of days to average for regression modeling varies (Webb et al.,
 364 2003). In addition to simple averages across varying numbers of days, other approaches include
 365 applying exponential weights (Koeh and Grünewald, 2010), we initially explored many metrics
 366 (Piotrowski and Napiorkowski, 2019; Soto, 2016) or including separate terms for air
 367 temperatures on the day of interest and preceding days (Siegel and Volk 2019). We tested five
 368 categories of air temperatures covariates in our models, where A_i is the i th day. In these initial
 369 explorations at Scott River, we found that two-day weighted air temperature (A_{2w}) resulted in
 370 good model fits (Text S2), so we used A_{2w} for all models except one that used a seven-day
 371 average (A_7) to mimic Mohseni et al.’s (1998) widely-implemented model. A_{2w} is calculated as
 372 follows, where A_i is mean air temperature on the day i , using Equations (1), (2), (3), (4), and (5):

373 Single-day average A_1 :

$$374 A_1 = A_i \quad (1)$$

376 Multi-day averages $A_2 \dots A_7$:

$$377 A_2 = \frac{(A_i + A_{i-1})}{2}, \dots, A_z = \frac{(A_i + A_{i-z} \dots A_{i-w})}{z} \quad (2)$$

379 Multi-day weighted averages A_{2w} and A_{3w} , with preceding days discounted by 50% per day:

$$380 A_{2w} = A_i + \frac{(0.5 \cdot A_{i-1})}{1.5} \text{ and } A_{3w} = \frac{(A_i + 0.5A_{i-1} + 0.25A_{i-2})}{1.75} \quad (3) = \frac{A_i + (0.5 \cdot A_{i-1})}{1.5} \quad (1)$$

383 Lagged averages A_{L3} and A_{L5} :

$$A_{L3} = \frac{(A_{t-1} + A_{t-2} + A_{t-3})}{3} \text{ and } A_{L5} = \frac{(A_{t-1} + A_{t-2} + A_{t-3} + A_{t-4} + A_{t-5})}{5} \quad (4)$$

Differences between lagged average and day i :

$$A_{\Delta3} = (A_t - A_{L3}) \text{ and } A_{\Delta5} = (A_t - A_{L5}) \quad (5)$$

To improve numerical stability, we standardized each air temperature ($^{\circ}\text{C}$) and flow predictor variable ($\log_{10} \text{ m}^3/\text{s}$) by centering and scaling (i.e., subtracting the mean) and scaling (i.e., then dividing by the standard deviation).

3.1.3 Flow and air temperature quantiles

At each site, we used smooth additive quantile regression models (Cade and Noon, 2003; Fasiolo et al., 2020) to calculate the air temperature associated with three quantiles (0.1, 0.5, and 0.9, equivalent to 10%, 50%, 90% exceedance probabilities) for each day of the year (Figure 3a), using the `qgam` R package (Fasiolo et al., 2020) with a 12-knot cyclic cubic regression spline (“cc”). We refer to the 0.1, 0.5, and 0.9 air temperature quantiles as Coolest, Typical, and Hottest, respectively. We also derived three flow quantiles, with the 0.1 quantile representing Lowest flows, 0.5 quantile representing Typical flows, and the 0.9 quantile representing Highest flows (Figure 3b). These quantiles were used to generate model scenarios (Section 3.4).

We used similar quantile regression models at each site to categorize each date into one of nine categories based on combinations of flow quantiles (High is >0.67 quantile, Moderate is 0.33 – 0.67 quantile, Low is <0.33 quantile) and air temperature quantiles (Cool is <0.33 quantile, Moderate is 0.33 – 0.67 quantile, Warm is >0.67 quantile). These categories were used to define cross-validation blocks (Section 3.3).

3.2 Model development and calibration

At each of the 10 sites, we developed statistical models to predict DMST of T_{\max} and $\text{DMST}_{\text{mean}}$ using combinations of river flow and air temperature, and day of year (D) as predictors/covariates, including interactions (Table 1). We tested three classes of models: non-linear logistic regression, harmonic regression, and generalized additive models (GAM). Models/GAMs were developed in R version 4.02 (R Core Team 2020).

3.2.1 Generalized additive models (GAMs)

We focused our stream temperature modeling on GAMs because they offer powerful flexibility including non-linear smoothers (Pedersen et al., 2019; van Rij et al., 2019). We used the `bam` function in the `mgcv` R package version 1.8-36 using the `bam` function (Wood, 2017) to develop GAM models, fit using fast restricted maximum likelihood (fREML). We also re-fit using maximum likelihood (ML) solely to obtain Bayesian information criterion (BIC) scores. Model terms can be either linear coefficients or smooth non-linear functions (Wood,

2017; Pedersen et al., 2019). The non-linear functions are smooth curves with the amount of wiggleness automatically determined by a smoothing penalty. (Pedersen et al., 2019; Wood, 2017). We used cyclic cubic regression splines (“cc”) as the smoother for day of the year D and thin plate regression splines (“tp”) as smoothers for other covariates. To improve prediction under new conditions and avoid overfitting (Jackson et al., 2018; Siegel and Volk, 2019), we limited smoothers for most variables air temperature and flow to a maximum of three knots, except D which in the one-covariate model “GAM11” where air temperature was allowed six knots. D was allowed up to six knots, except in three-dimensional tensors where it was restricted to five knots.

We compared GAMs that some models included interactions between D and other covariates (i.e., flow or air temperature) to allow the relationships between covariates and the response variable to that covariate’s effect to vary seasonally to GAMs where those relationships are seasonally constant. Our GAM models represented interactions between variables as. These interactions were either partially non-linear or fully non-linear. For a partially non-linear interaction, the linear slope of one variable (e.g., flow) changed as a smooth non-linear function of another variable (i.e., D), an approach used by (Jackson et al., 2018) and Siegel, Siegel and Volk (2019) and specified in `mgev` using the “by” option. Fully non-linear relationships between two or more variables were specified as tensor product smooths in `mgev` using the syntax “te()” (Wood, 2017). If main effects were included as separate terms, then we used “ti()” to specify or tensor product interactions (Wood, 2017).

All our GAM models included a random effect for year and all but one (“except “GAM11,” Section 4.2), the simplest model structure tested, included an AR-1 autocorrelation error structure. The `bam` function cannot automatically derive the AR-1 coefficient (ρ), so it must be manually assigned. Following Baayen et al. (2018) and van Rij et al. (2019, 2020), and a random effect for year. We initially fit each model without an autocorrelation term, and then re-ran the model fit with an autocorrelation term, assigning a ρ value based on the initial model’s lag-1 autocorrelation from the residuals of the initial model. (Baayen et al., 2018) and van Rij et al. (2019) advise testing several ρ values using model comparison procedures, which in our case always confirmed the initial values were optimal. (2020) (Text S3).

3.2.2 Harmonic regression

As an alternative to compare to GAMs, we use harmonic regression (also known as trigonometric or periodic regression) (Cox, 2006) with paired sine and cosine interaction terms that allow the slope of covariates to vary as a smooth cycle over the course of the year (Bodeker et al., 1998). For daily periodicity, we multiplied day of the year D by $2\pi/365$ (Helsel et al., 2020). We developed these models using the `lme` function in the `nlme` R package version 3.1-148 (Pinheiro et al., 2020) with an AR-1 autocorrelation term and a random intercept for year, fit using maximum likelihood (ML). Harmonic regression of stream temperature is common (Kothandaraman, 1971; Johnson et al., 2020), but we are not aware of previous applications of harmonic interactions between D and other covariates for stream temperatures.

3.2.3 Non-linear logistic regression

Since Mohseni et al.'s (1998) non-linear logistic regression of weekly air temperature and stream temperature has been so widely applied, we use it as a benchmark to compare our other model to. Many streams, including the Scott River (Manhard et al., 2018), exhibit hysteresis in which the relationship between stream temperature and air temperature differs between spring and fall (Mohseni et al., 1998). Following Jones et al.'s (2016) code using R's `optim` function, we modeled the ascending (weeks 1–30) and descending (weeks 31–52) limbs separately, fitting models using weekly averages and then apply them to daily data. These models do not include flow, autocorrelation, or random effects. We used 7-day average air temperatures to match the original method widely applied and adapted (Piotrowski & Napiorkowski, 2019), we included a GAM equivalent of it as a benchmark for comparison. A_7 is the only predictor in this “GAM11” model (i.e., no flow, autocorrelation, or random effects).

We reviewed residual plots and autocorrelation function plots to verify assumptions. We evaluated each model's concurvity using `mgcv`'s concurvity function.

3.3 Model selection and validation

We compared alternative model configurations (which variables and interactions are included, which are assigned random effects, etc.) to select a final model (Table 1). Initial exploration indicated that $A_{2,w}$ (2-day weighted air temperature) provided better model fits than other air temperature variables, so we used $A_{2,w}$ for most of our models. After final model selection, we developed a separate set of models to assess the sensitivity of model fits to using different air temperature variables (Figure S1). Rather than slavishly follow a pre-specified procedure such as forward selection or backward selection, we took a more holistic approach to model selection. We selected a final model after considering multiple models using a variety of methods including Akaike information criterion (AIC), `fREML` (fast restricted maximum likelihood) scores for GAMs, goodness of fit metrics (root mean squared error [RMSE] and coefficient of determination [R^2]), and review of residual plots and auto-correlation function plots. Concurvity, the non-linear equivalent of collinearity, is a potential concern for GAMs such as ours that contain smooths for time along with other time-varying covariates (Amodio et al., 2014; Wood, 2017), so we evaluated each GAM's concurvity using `mgcv`'s concurvity function.

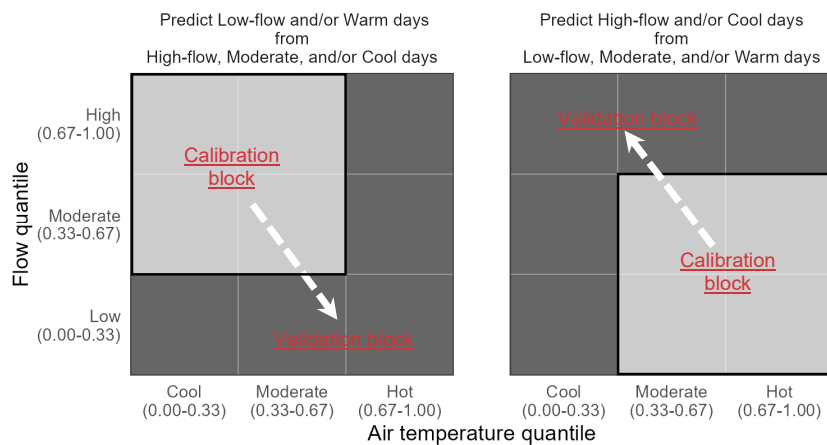
Prior to modeling, we randomly selected and excluded all data from 4 (17%) of the 24 years. These data were not used in model selection but instead were retained for out-of-sample validation.

We validated models using two methods. First, we used leave-one-year-out (LOYO) cross-validation, a version of k -fold variation in which we withhold a year, re-fit the model using the 19 remaining years, compare predictions for the withheld year against the measured data using goodness of fit metrics (RMSE and R^2), and then repeat the same process for each year. Second, for out-of-sample validation, we compared model predictions (calibrated with 20 years of data) against data from the four removed years using goodness of fit metrics (RMSE and R^2).

3.5 We used cross-validation (CV) for model selection and validation because it is preferred over information theoretic approaches when prediction is paramount (Pedersen et al., 2019). We

505 designed extrapolation CV tests to select models that performed well when applied to
 506 environmental conditions (i.e., flow and air temperature) outside the calibration range (Lute &
 507 Luce, 2017; Roberts et al., 2017). We split data into blocks based on quantiles of flow and air
 508 temperature (Section 3.1.3), withheld one block, and fit the model using the remaining block
 509 (Figure 4). We compared predictions for the withheld block against the measured data using root
 510 mean squared error (RMSE). These dual-variable differential split-sample tests (Klemeš, 1986)
 511 extrapolate not only into new combinations of flow and air temperature but also into new ranges
 512 of both individual variables.

513 We selected the final model by averaging all 40 RMSE values from extrapolation tests (10 sites
 514 × 2 extrapolation tests × 2 parameters [T_{max} and T_{mean}]) and choosing the model with lowest
 515 mean RMSE. We selected the same model structure for T_{max} and T_{mean} (rather than optimizing
 516 separately) so predictions for both metrics could be used together. We present BIC scores to
 517 compare our extrapolation-based model selection to more commonly applied model selection
 518 methods. To facilitate comparisons to previous studies, we also use leave-one-year-out (LOYO)
 519 CV where data were split into annual blocks and then treated similarly to the extrapolation tests
 520 (i.e., steps repeated for each year: year withheld, model refit using remaining data, and
 521 predictions compared to withheld data). We assessed the relative importance of individual model
 522 terms by comparing performance among models with and without individual predictors and/or
 523 interactions.



526 **Figure 4.** Configuration of data blocks used in extrapolation tests for model selection and
 527 validation.
 528
 529
 530

3.4 Model application to hydroclimatic and flow scenarios assessing management scenario effects and timing of flow importance

3.4.1 All sites

To assess the seasonal response of stream temperatures to variation in flow and air temperatures, we applied our selected GAM models to a group of 15 model to scenarios representing differing air temperatures and flows (Table 2, Figure 3). We ran nine “quantile air temperature” scenarios representing combinations of 3 air temperature inputs and 5 flow inputs (Table 2, Figure 3). All three air temperature inputs were derived using non-parametric quantile regression (Cade and Noon, 2003; Muggeo et al., 2013) to calculate the air temperature associated with three quantiles (0.05, 0.50, and 0.95, equivalent to 5%, 50%, 95% exceedance probabilities) for each day of the year (Figure 3a), using the `quantregGrowth` R package (Muggeo et al., 2013), with options described in Text S3. For air temperature, the 9 quantiles and three flow inputs (0.50 quantile represented typical conditions, the 1, 0.05 quantile represented hottest conditions, and the 5, and 0.95 quantile represented coolest conditions. Three of the five flow inputs were based on quantiles (0.05, 0.50, and 0.95) derived using similar methods as the air temperature inputs, with the 0.50 quantile representing typical conditions, the 0.05 quantile representing very low flow conditions, and the 0.95 quantile representing high flow conditions (Figure 3b). The remaining two of the five 9 quantiles (Section 3.1.3) for each site. Replication is sparse for the co-occurrence of extreme quantiles of both air temperature and flow inputs are based on the USFS water right and California Department of Fish and Wildlife (CDFW) Interim Instream Flow Criteria. The USFS first priority Scheduled D water right varies by (e.g., mean 4.9 days of record per month and day, from a high of 200 ft³/sec (5.67 m³/sec) in November through March to a low of 30 ft³/sec (0.85 m³/sec) in August and September (Superior Court of Siskiyou County, 1980) (Figure 3b). The CDFW criteria vary by site with flow <0.1 quantile and air temperature >0.9 quantile; however, ample data are available in nearby quantiles (e.g., mean 19.1 days per month and day, from a minimum of 62 ft³/sec (1.75 m³/sec) in September to a high of 362 ft³/sec (10.3 m³/sec) in February (CDFW, 2017) site with flow <0.2 quantile and air temperature >0.8 quantile (Figure 3b) S1).

3.4.2 Scott River

At Scott River only, six additional scenarios were run that paired the three quantile air temperatures with the USFS water right and CDFW flow criteria (Section 2) as flow inputs (Table 2, Figure 3). The CDFW and USFS flows do not follow a particular flow quantile through the entire year, but instead are aligned with extreme drought conditions in April and May (0.05 quantile) and high flows in August and September (0.50 to 0.95 quantile).

To assess the realistic timing and magnitude of modeled exceedances of stream temperature thresholds, We also applied our selected GAM model to predict stream temperatures in a group of “observed air temperature” scenarios that pair the observed daily air temperature time series temperatures for 1995–1998–2020 with eight flow conditions for the Scott River: observed USGS flows in addition to the five flows used in the “quantile air temperature” scenarios (low, typical, high, USFS, and CDFW) as well as two additional scenarios in which the CDFW and USFS, the five flows are used as minimums that are supplanted from the “quantile air temperature” scenarios (Lowest, Typical, Highest, USFS, and CDFW), and two additional

574 ~~scenarios in which the CDFW and USFS flows were replaced~~ by observed USGS flows on dates
575 when the observed flows ~~are were~~ higher ~~than the management flows~~ (Table 2). ~~We expect that~~
576 Using observed air temperatures instead of quantile air temperatures provides more realistic ~~real-~~
577 ~~world~~ predictions because air temperatures fluctuate ~~erratically~~ from day to day (Figure 22a),
578 instead of ~~staying remaining~~ near the same quantile like flow does during ~~the seasonal flow May-~~
579 ~~September recession each year from May through September.~~

580 . We summarized the results of each “observed air temperature” scenario by calculating: 1)
581 annual maximum temperature, 2) first and last day each year in which water temperatures exceed
582 22 °C, and 3) the annual degree days exceedance of 22 °C, calculated by subtracting 22 from all
583 ~~DMxSTT_{max}~~ and summing all positive values ~~by year~~. We chose 22 °C as an indicator of
584 biological effects on juvenile salmonids ~~that rear in the mainstem Scott River or outmigrate~~
585 ~~downstream using the river as a migratory corridor. Given the potential for local genetic~~
586 ~~adaptation to thermal regimes (Zillig et al., 2021), we prioritized, based on geographically~~
587 ~~proximal studies near the Scott River in selecting thresholds. When the Klamath River exceeds~~
588 ~~22–23 °C, juvenile salmonids move to tributary confluences (Brewitt & Danner, 2014; Sutton et~~
589 ~~al., 2007; Sutton and Soto, 2012; Brewitt and Danner, 2014). Similar behavior was observed~~
590 ~~in the Shasta River (Nichols et al., 2014) and 22 °C was also used by McGrath et al. (2017). The~~
591 ~~22 °C threshold is not fully protective for coho salmon (Text S4) but we chose it because our~~
592 ~~study site is a mainstem river where temperatures are expected to be higher than a cool~~
593 ~~tributary.).~~

594
595

Table 1. Comparison List of Scott River GAMs and model training statistics.

Model Name	Predictor variables	Daily maximum stream temperature (DMsST _{Lmax})						Daily mean stream temperature (DMST _{Lmean})					
		REM	AIC	ARI	edf _g	RMS		REM	AIC	ARI	edf _g	RMS	
		L-BIC	ARI	edf _r	df _R	E	R ²	L-BIC	ARI	edf _r	f _R	E	R ²
GAM1: tensor Q-A _{2w} -D	te(Q, A _{2w} , D)	5004 ₁₂	9901	0.58	46.5	0.861	0.982	335485	0.659	0.74	46.51	0.778	0.979
		830	0.526	723.	18.1	06	973	62	6607	722.	8.1	0	978
				6						8			
GAM2: tensors Q-D & A _{2w} -D	s(A _{2w}) + ti(A _{2w} , D) + te(Q, D)	5036 ₁₂	9973	0.60	36.4	0.881	0.981	336484	6639	0.76	35.61	0.80	0.978
		734	0.529	318.	18.0	05	974	92	0.667	917.	8.0		979
				4						1			
GAM3: tensor Q-D & vary A _{2w}	s(D, by = A _{2w}) + s(A _{2w}) + te(Q, D)	5039 ₁₂	9978	18.0	39.3	0.861	0.982	337384	6649	0.74	39.11	0.758	0.980
		745	0.531	580	18.0	05	974	82	0.672	216.	8.0	0	978
				1						3			
GAM4: tensors Q-D & A _{2w} -Q <i>(final)</i>	s(D, by = A _{2w}) + s(A _{2w}) + ti(A _{2w} , Q) + te(Q, D)	5053 ₁₂	1002	0.60	36.3	0.891	0.981	340184	6729	0.76	35.41	0.80	0.978
		717	20.53	317.	17.9	05	974	86	0.671	316.	8.0		
				1						9			
GAM5: tensor tensor Q-D & no vary A _{2w} -Qv2	s(A _{2w}) + ti(A _{2w} , Q) + te(Q, D)	5095 ₁₂	1011	0.60	34.1	0.901	0.989	345284	6840	15.6	33.21	0.828	0.977
		724	60.53	815.	17.9	06	74	56	0.679	0.76	7.9	0	978
				7						4			
GAM6: tensor Q-D no vary Q & A _{2w} linear	s(D, by = A _{2w}) + te(s(D, by = Q) + s(D))	5105 ₁₂	1013	0.61	30.4	0.901	0.989	346685	6873	0.77	28.61	0.838	0.976
		828	90.57	113.	17.8	12	70	94	0.728	10.9	7.3	9	973
				8						9			
GAM7: varying vary Q & A _{2w} <i>(final)</i>	s(D, by = A _{2w}) + s(D, by = Q) + s(D, by = Q) + s(D)	5160 ₁₂	1025	12.6	28.2	1.070	0.978	346485	6871	0.80	27.51	0.888	0.973
		754	40.54	0.65	17.9	96	973	38	0.695	411.	7.6	4	976
				4						8			
GAM8: A _{2w} vary Q & no varying vary A _{2w}	s(A _{2w}) + s(Q) + s(D, by = Q) + s(D)	5448 ₁₂	1085	0.77	23.1	1.350	0.956	362685	7208	0.83	23.81	1.080	0.969
		736	50.55	312.	17.8	8	973	26	0.704	411.	7.5	84	76
				2						8			
GAM9: A _{2w} no Q or varying vary	s(A _{2w}) + s(Q) + s(D)	5525 ₁₃	1101	0.84	22.3	1.703	0.931	374987	0.764	0.87	21.17	0.961	0.941
		105	00.67	68.4	17.6	2	959	38	7459	58.1	6	30	969
				3									
GAM10: A ₂ only with ARI	s(A ₂)	6606	1318	0.88	21.3	2.75	0.817	5044	1006	0.905	21.2	2.29	0.819
				6						2			

<i>GAM11: A7 only</i>	$A_{2w} \sin(D) + s(D)$	104411	2082	N/A	23.2	2.211	0.882	933091	1860	N/A	23.11	1.742	0.895
<i>AR1</i>	or vary	3313	30.78	6.0	17.3	62	938	50	20.84	6.0	6.6	0	952
<i>Harmonic12: varying Q & A2w</i>	$A_{2w} + A_{2w} \sin(Dn) + A_{2w} \cos(Dn) + Q + Q \sin(Dn) + Q \cos(Dn) + \cos(Dn) + \sin(Dn)$	N/A	1036	0.73	N/A	1.04	0.969	N/A	6810	0.859	N/A	0.94	0.964
<i>Logistic13: Mohseni</i>	<i>GAM11: Logistic regression with $A_{7s}(A_7)$</i>	N/A	22	N/A	N/A	N/A	2.344	0.868	N/A	20	N/A	N/A	0
<i>A7 only no AR1</i>		668		5.8	0	0	865	265		5.8		8	882

596 *Note: GAM Models are sorted by $f_{REML} \text{ score} / \text{edf}_F$ for $DM \times ST \cdot T_{max}$, from most complex (GAM1) to least complex (GAM11).*
 597 *Except 'GAM11 A7 only no AR1', all GAM and LMM models also include an AR1 autocorrelation structure and a random effect of*
 598 *year. For models with italicized names, validation statistics are provided in Figures 4 (DMxST) and S5 (DMST). D = day of year from*
 599 *1 (1 January) to 366 (31 December in leap year), Q = daily mean flow in units of m^3/s , see Section 3.1.122 for key to 'A' air*
 600 *temperature variables, 's()' is a non-linear function, 's(D, by =)' is a linear interaction that varies smoothly by D, 'te()' is a fully non-*
 601 *linear tensor product smooth of two or three variables, 'ti()' is a tensor product interaction, ':' is linear interaction, $n = 2\pi/365$, f_{REML}*
 602 *= fast restricted maximum likelihood score, AIC = Akaike BIC = Bayesian information criterion score, AR1 = autocorrelation*
 603 *coefficient, edf_{edf}_F = effective degrees of freedom (edf) for fixed effects, edf_R = edf for random effects, RMSE = root mean squared*
 604 *error, of model training fit (not CV), and R^2 = coefficient of determination from model training fit (not CV).*

605 **Table 2.** Matrix showing the 23 stream temperature model scenarios representing combinations
 606 of air temperature and flow inputs, and organized into two scenario groups. The first group (15
 607 scenarios in Group 1 use) used “quantile air temperature” inputs (6 were only run only at Scott
 608 River while 9 were run at all Klamath Basin sites) and the second group (8 scenarios in Group 2
 609 use) were run only at Scott River and used “observed air temperature” inputs.
 610

Scenario group	Air temperature inputs	Flow inputs							Observed
		Lowest (0.051 quantile)	Typical (0.505 quantile)	Highest (0.959 quantile)	USFS water right	CDFW flow criteria	Observed	Maximum of observed or USFS as minimum	
Quantile air temperature	Hottest (0.959 quantile)	Group 1 All sites	Group 1 All sites	Group 1 All sites	Group 1 Scott only	Group 1 Scott only			
	Typical (0.505 quantile)	Group 1 All sites	Group 1 All sites	Group 1 All sites	Group 1 Scott only	Group 1 Scott only			
	Cooltest (0.051 quantile)	Group 1 All sites	Group 1 All sites	Group 1 All sites	Group 1 Scott only	Group 1 Scott only			
Observed air temperature	Group 2 Observed (measured on date)	Group 2 Scott only	Group 2 Scott only	Group 2 Scott only	Group 2 Scott only	Group 2 Scott only	Group 2 Scott only	Group 2 Scott only	Group 2 Scott only

Inserted Cells

Deleted Cells

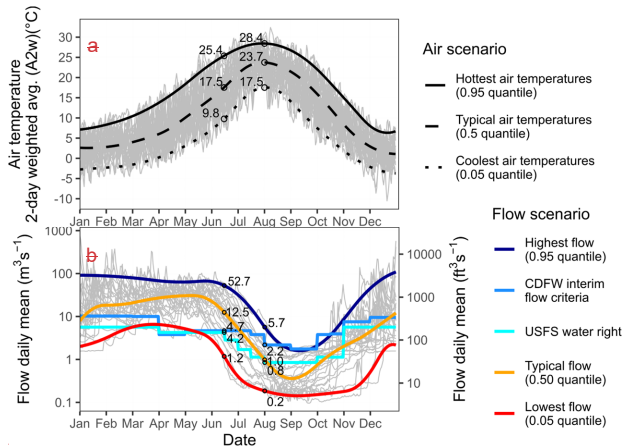
Split Cells

Inserted Cells

Inserted Cells

Inserted Cells

611 *Note:* USFS = USFS Schedule D first priority water right (Superior Court of Siskiyou County,
 612 1980), and CDFW = CDFW Interim Instream Flow Criteria (CDFW, 2017). See text for
 613 explanation of quantiles and flow minimums.
 614
 615
 616



617
 618 **Figure 3.** Inputs to Group 1 scenarios representing 15 combinations of (a) three air temperature
 619 inputs and (b) five flows inputs that vary by day. Observed values for 1995–2020 are shown as
 620 gray lines in both panels. Data values are labeled for 15 June and 1 August.
 621

622 **4 Results**

623 **4.1 Measured water temperature, air temperature, and flow**

624 From May–July, measured water temperatures were highly variable among years (Figure 2). For
 625 those months, the highest flow years had DMxST averaging 6.8 °C cooler than during lowest
 626 flow years, while DMST averaged 5.3 °C cooler. In contrast, from August through October inter-
 627 annual differences in water temperature much less pronounced. Annual maximum water
 628 temperatures occurred earlier in the season in low flow years (i.e., early/mid July) than in high
 629 flow years (i.e., late July or early August). These observations inspired us to develop seasonally
 630 varying models.

631
 632 **4.2 Model selection and validation**

633 In extrapolation CV of the 11 models (Table 1), GAM7 had the lowest all-site mean RMSE (T_{\max}
 634 1.13 °C, T_{mean} 1.00 °C), as well as the lowest RMSE for Scott River (T_{\max} 1.20 °C, T_{mean} 1.00
 635 °C), so was selected as our final model (Figure 5). GAM7 features nonlinear smoothers for day
 636 of year (D), two-day weighted air temperature (A_{2w}), and flow (Q); a nonlinear smoother of D
 637 interacted with linear Q (i.e., linear slope of Q varies by D); and a nonlinear smoother of D
 638 interacted with linear A_{2w} (Table 1, Figure S3, Figure 6). GAM7 has intermediate complexity,
 639 with 12.6 effective degrees of freedom for fixed effects (edf_f) for Scott River T_{\max} , compared to
 640 23.6 for the most complex model (GAM1), and 5.8 for the least complex model (GAM11) (Table
 641 1).

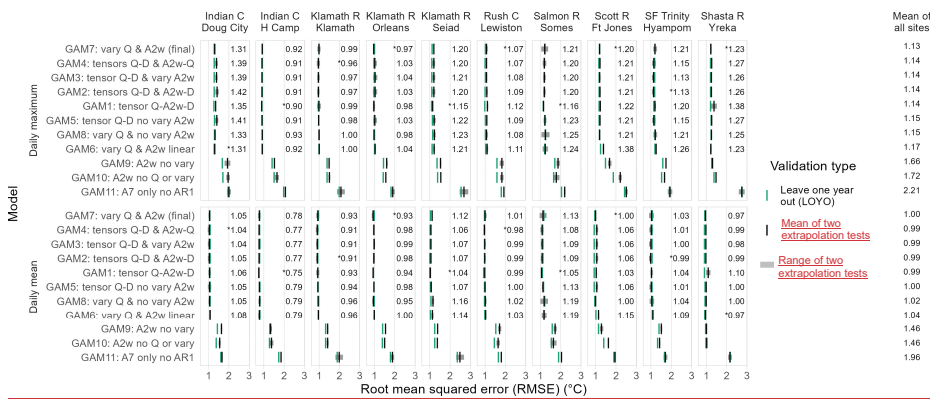
642 Extrapolation CV showed that at all sites, including Scott River, models with seasonally varying
 643 flow effects had much higher accuracy than models lacking that feature (Figure 5). For example,

644 for T_{max} , all-site RMSE was 1.13–1.17 °C for models with seasonally-varying flow effects
 645 (GAM1–GAM8) and 1.66 °C for GAM9 that lacked seasonally varying flow. Models lacking
 646 flow (i.e., containing only D or A_{2w}) performed the worst, with all-site RMSE values of 1.72 °C
 647 and 2.21 °C for GAM10 and GAM11, respectively, for T_{max} . GAM7’s combination of a
 648 nonlinear smoother for flow and a partially nonlinear interaction of flow and D represented flow
 649 effects well, given that the additional complexity of tensors (fully nonlinear interactions of flow
 650 and D) in GAM1–GAM5 did not substantially improve model performance at most sites. Models
 651 interacting flow and air temperature (i.e., GAM1 and GAM4) did not outperform GAM7 which
 652 lacked this interaction.

653 BIC scores (Figure S4) largely corroborate the extrapolation CV results identifying the
 654 importance of seasonally varying flow effects. Of eight models with seasonally varying flow
 655 effects, the most complex model (three-way tensor GAM1) had the worst overall (averaged
 656 across all sites) BIC score, but intermediate extrapolation CV RMSE. Averaging BIC ranks
 657 across sites, our extrapolation CV-selected model, GAM7, had the best BIC ranks for both T_{max}
 658 and T_{mean} (Figure S4); however, at many individual sites including Scott River, other models had
 659 better BIC scores (Figure S4, Table 1).

660 Scott River GAM7 LOYO CV predicted overall seasonal patterns in measured T_{max} for dates
 661 stratified into combinations of differing quantiles of air temperatures and flows. RMSE was
 662 higher for dates with low (<0.33 quantile) flows (Figure S2c). T_{max} Scott River GAM7
 663 extrapolation CV prediction accuracy was only slightly lower than LOYO CV prediction
 664 accuracy when averaged over the entire year (i.e., RMSE 1.20 °C vs. 1.18 °C, Figure 5), but
 665 were biased low during May and June during high (>0.67 quantile) flows, having only been
 666 calibrated with data from the low-flow and moderate-flow quantile (Figure S5). Complete time
 667 series of Scott River measured and LOYO CV T_{max} and T_{mean} for all years are shown in Figures
 668 S6–S7.

669
 670



671

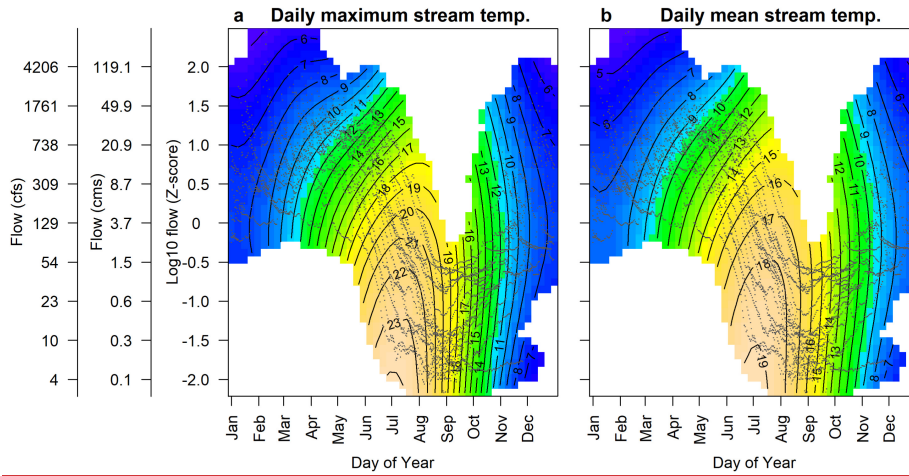
672 **Figure 5.** The sensitivity analysis of model training statistics for models using various air
 673 temperature metrics indicated similar performance for most of the metrics, except the longest
 674 multi-day air temperature averages which had higher RMSE (Figure S1). For DMxST, RMSE

675 ranged from 0.88–0.90 °C for all air temperature metrics except the 3-day to 7-day averages
676 which were 0.96–1.15 °C (Figure S1). For DMST, RMSE ranged from 0.79–0.82 °C for all air
677 temperature metrics except the 4-day to 7-day averages which were 0.85–0.98 °C and the single-
678 day average (0.87 °C) (Figure S1). Given the excellent performance of the 2-day weighted air
679 temperature (A_{2w}) in predicting both DMxST and DMST (Figure S1), we use A_{2w} for all models
680 except Logistic13 and the two GAM models that mimic it (Table 1).

681 Validation and training statistics indicate a wide range of performance (Table 1, Figure 4), with
682 the tensor models (i.e., GAM1, GAM2, GAM3, GAM4, GAM5, GAM6) performing best while
683 those models that used only Summary of RMSE from extrapolation and LOYO CV tests at 10
684 Klamath Basin sites applying T_{max} (top panels) and T_{mean} (bottom panels) models to years
685 (LOYO) or flow and air temperature combinations (extrapolation) not used in model calibration.
686 Models are sorted by overall RMSE (i.e., mean of all 10 sites and both temperature metrics).
687 Data labels for top eight models in individual site panels are means from extrapolation tests, with
688 asterisk marking lowest RMSE in each panel. Labels at right edge of graph are all-site means for
689 each model and parameter.

675
676
677
678
679
680
681
682
683
684
685
686
687
688
689
690

691



692

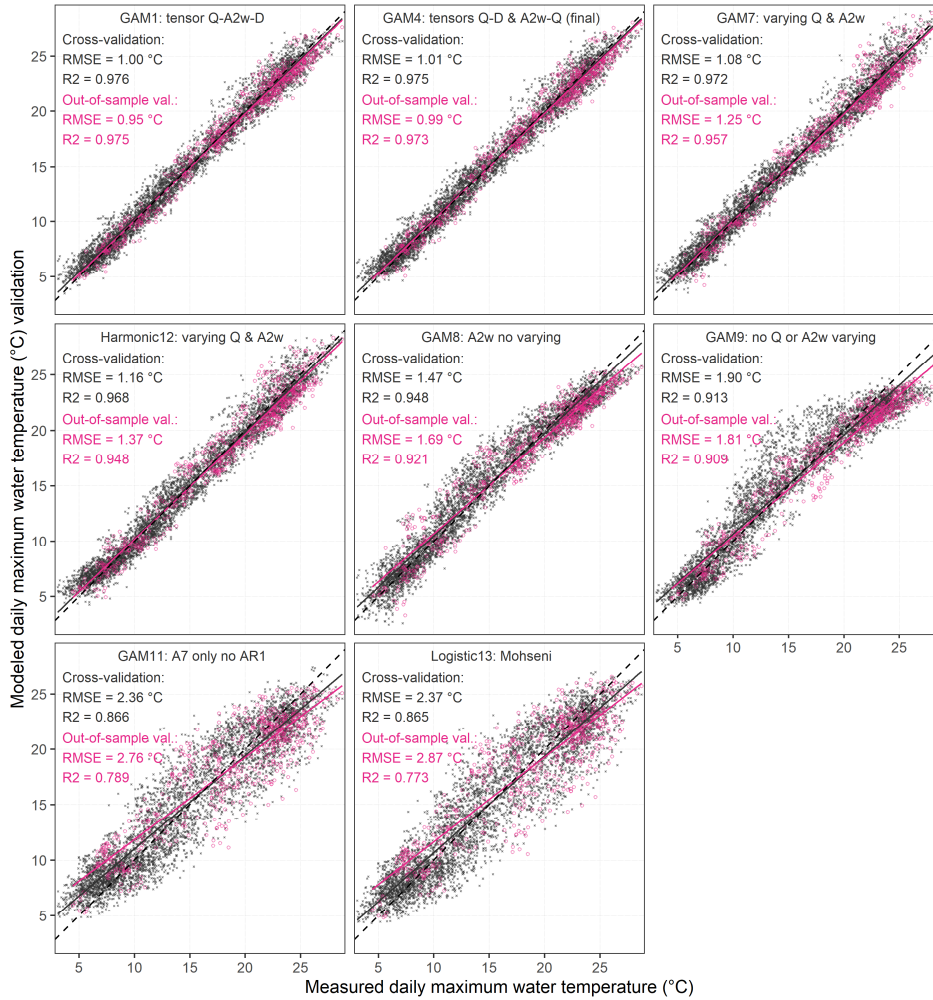
693 **Figure 6.** Effects of flow (Q) and day of year (D) on predicted values of (a) T_{\max} and (b) T_{mean} in
694 Scott River GAM7. Colors and labeled contour lines show predicted temperatures ($^{\circ}\text{C}$).
695 Underlying gray dots show calibration data.

696

697 4.2 Model scenarios assessing management effects and timing of flow importance

698 Water temperature predictions under quantile air temperature (e.g., Logistic13 and its GAM
699 equivalent GAM11) performed scenarios on the worst.

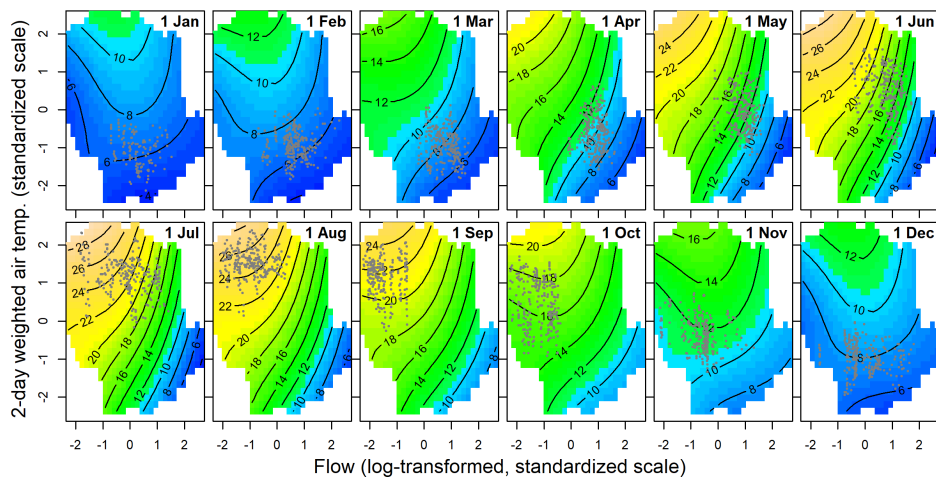
700 GAM4, chosen as Scott River using our selected model for reasons discussed in Section 5.1, had
701 a cross-validated RMSE of 1.01 °C for DMxST (Figure 4) and 0.93 °C for DMST (Figure S5),
702 with similar values for out-of-sample validation. Similar to the measured data (Figure 2), in the
703 May–July period the selected model predicts cool (GAM7) showed water temperatures during
704 high-flow years and warm water temperatures during low-flow years (responded to changes in
705 flow across all quantiles of air temperature, consistent with measured data (Figure S2). The
706 effects plot for the selected models show that stream temperatures are relatively insensitive to
707 flow from 1 December to 1 March, but that flow exerts a strong cooling influence from 1 April
708 to 1 August (Figure 5, Figure S7). The complete time series of measured and modeled water
709 temperature data for all years is available as Figure S3 and S4 for DMxST and DMST,
710 respectively.



711
 712 **Figure 4.** Comparison of measured DMxST to LOYO cross-validation predictions and out-of
 713 sample validation predictions for 1995–2020. Solid lines are linear regression and dotted lines
 714 are the 1:1 (Y=X) lines.
 715

716

717



718

719 **Cooling effects of** **Figure 5.** Effects plot showing predictions from selected model “GAM4:
720 tensors Q-D & A2w-Q” that uses 2-day weighted air temperature (A_{2w}), flow (Q), and day of
721 year (D) as predictors. Colors show predicted DMxST as function of Q and A_{2w} , with DMxST
722 labeled contour lines spaced 2 °C apart. Panels represent the first day of each month. Gray dots
723 show position of calibration points within 5 days of first of each month.
724

725

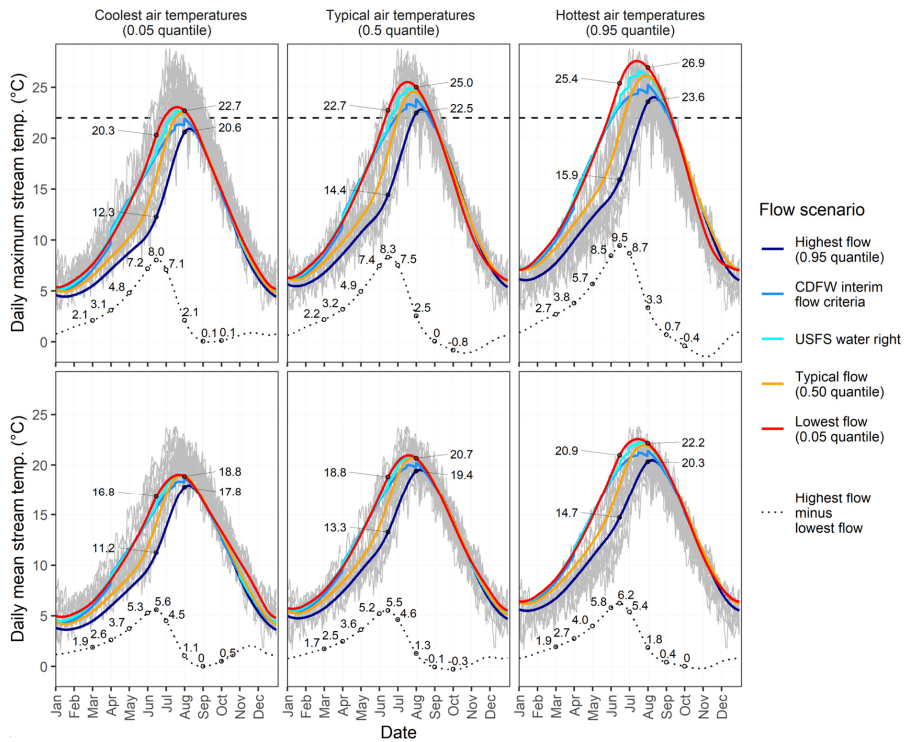
726 **4.3 Model application to hydroclimatic and flow management scenarios**

727 The “quantile air temperature” model scenarios show that flow and air temperature both had
 728 strong effects on water temperature (Figure 6). The cooling effect of high flow followed a
 729 seasonal pattern, rising in March to reach a peak maximum effect size on 15 June (up to 9.5 °C
 730 for DMxST and 6.27.7 °C for DMST_{T_{max}} and 5.5 °C for T_{mean}), then diminishing to near zero by
 731 early September (Figure 6). Cooling effects of high flows were stronger when air temperatures
 732 were high than when air temperatures were low (e.g., 15 June difference in DMxST between
 733 highest flow and lowest flow scenarios is 9.5 °C with the hottest air temperatures and 8.0 °C
 734 with the coolest air temperatures). With less solar radiation (due to shorter days and lower solar
 735 angle) and lower air temperatures than earlier months, DMxST is almost always less than 22 °C
 736 by early September regardless of flow (gray lines in top panels of Figure 6). Consistent with
 737 the measured data (Figure 2S2), modeled annual maximum water temperatures occurred later in
 738 the season in high-flow years/conditions (i.e., late July or early August) than in low-flow
 739 years/conditions (i.e., early/mid-July) (Figure 67).

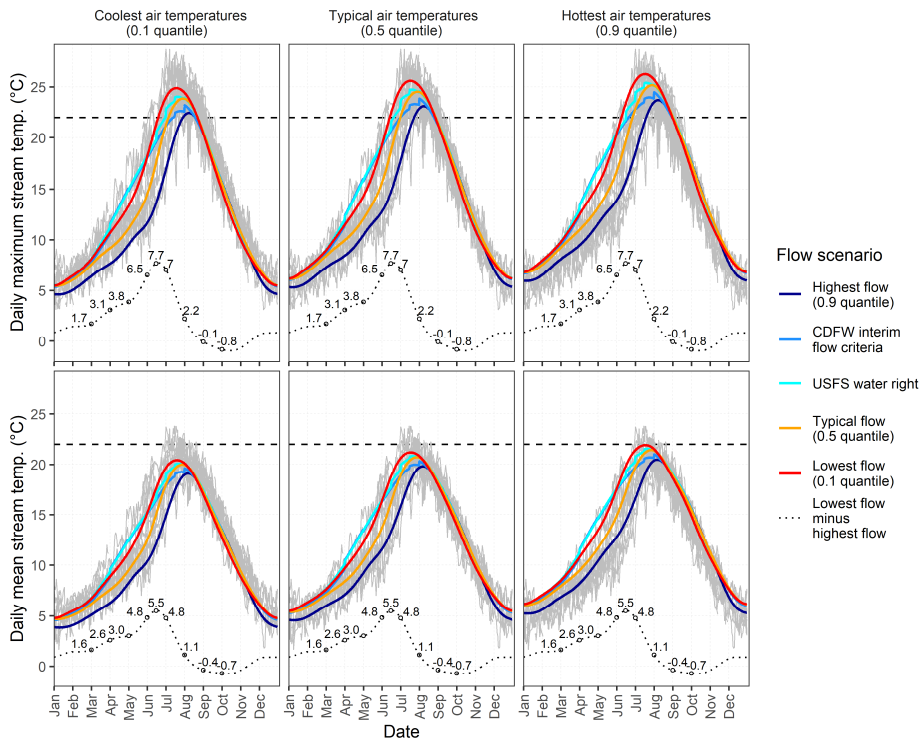
740 In the Timing and magnitude of flow effects varied among the 10 Klamath Basin sites, but
 741 generally followed a similar seasonal trend of flow having the strongest cooling effects in April–
 742 July, less cooling effects in March and August, and warming effects in November through
 743 February (Figure 8). Cooling effects of flow were strongest at Scott River and weakest at Shasta
 744 River.

745 The Scott River “observed air temperature” scenarios, we modeled DMxST pairing the which
 746 paired observed air temperature time series for 1995–2020 with eight flow scenarios (Table 2,
 747 Figures 7 and S8). These scenarios provide an indication of the range (e.g., due to air
 748 temperatures) in daily water temperature associated with each temperatures with eight flow
 749 scenarios, demonstrated how flow variation influences stream temperature timing and
 750 magnitude. The lowest flow scenario. Compared to the lowest flow scenario (0.05 quantile), the
 751 highest flow scenario (0.95 quantile) has (0.1 quantile) had annual maximum temperatures that
 752 are 3.73 °C cooler/warmer than the highest flow scenario (0.9 quantile) (Figure 7a)9a), and
 753 temperatures first reach/reached 22 °C 54/48 days later/earlier (Figure 7e); in contrast, there is only
 754 a 2-day difference in 9c). The last day of the year that has with temperatures >22 °C differed by
 755 only 2 days (Figure 7d)9d). The scenario with observed flows has scenario had the most
 756 interannual variation in the annual maximum temperature (Figure 7a)9a) and timing of
 757 exceedances of 22 °C (Figure 7e)9c,d), because it includes/included very low flows as well as and
 758 very high flows. Water/Predicted temperature responses to the CDFW and USFS flow scenarios
 759 are complex and depend on how the flows are implemented. If implemented as bypass flows,
 760 above which all additional water is diverted, then temperatures reach/reached 22 °C 17 days
 761 earlier with the exact USFS flows than with the observed flows flow scenario by 4 days for the
 762 CDFW flows and 13 days for USFS flows (Figure 7e)9c and Figure S8) because the USFS these
 763 management flows are much lower than average-observed flows in May and June. In contrast
 764 (Figure 3). However, in the scenario in which scenarios where the CDFW and USFS flows are
 765 treated as minimums (supplanted/were replaced by observed USGS flows on days/dates when the
 766 observed flows are higher), temperatures reach 22 °C on the same day as the observed flow
 767 scenario (Figure 7d). Due to high July and August flows in the CDFW scenarios, annual
 768 maximum water temperatures are 1.1–1.3 °C cooler in the CDFW scenarios than the observed
 769 flow scenario (Figure 7a). Relative to the observed flow scenario, the date that the CDFW as

770 minimum scenario first reaches 22 °C is only 3 days later average (2 July vs. 30 June), but were
 771 higher than the management flows, then predicted temperatures reached 22 °C later than the
 772 observed scenario by 4 days with CDFW flows and 2 days with USFS flows. In addition, the
 773 number of years with exceedances of 22 °C prior to 23 June 20 were reduced from 67 to 20
 774 (Figure 7e9c) because the CDFW flows were higher than observed flows in drought years.
 775 Patterns of inter-scenario
 776 temperatures were 1.0–1.1 °C cooler in the CDFW scenarios than the observed flow scenario
 777 (Figure 9a). Differences in annual degree-days exceedance of 22 °C between scenarios (Figure
 778 7b) are very 9b) were similar to those of annual maximum temperature (Figure 7a). While the
 779 CDFW flows and USFS flows are both predicted to improve (i.e., cool) summer temperatures
 780 relative to current conditions, these improvements would be greater with the higher CDFW
 781 flows.



782
783



784

785 **Figure 6.** Predicted maximum T_{max} and mean water temperatures T_{mean}
 786 under the 15 “quantile air temperature” scenarios representing combinations of three air
 787 temperature inputs (arranged in columns) and three quantile flow inputs and two management
 788 flow inputs (shown by color). Observed values for 1995–2020 are shown as gray lines.
 789 Selected data values are labeled on 15 June and the first day of the months March–October.
 790 Horizontal dashed line at 22 °C T_{max} is the salmonid temperature threshold.
 791

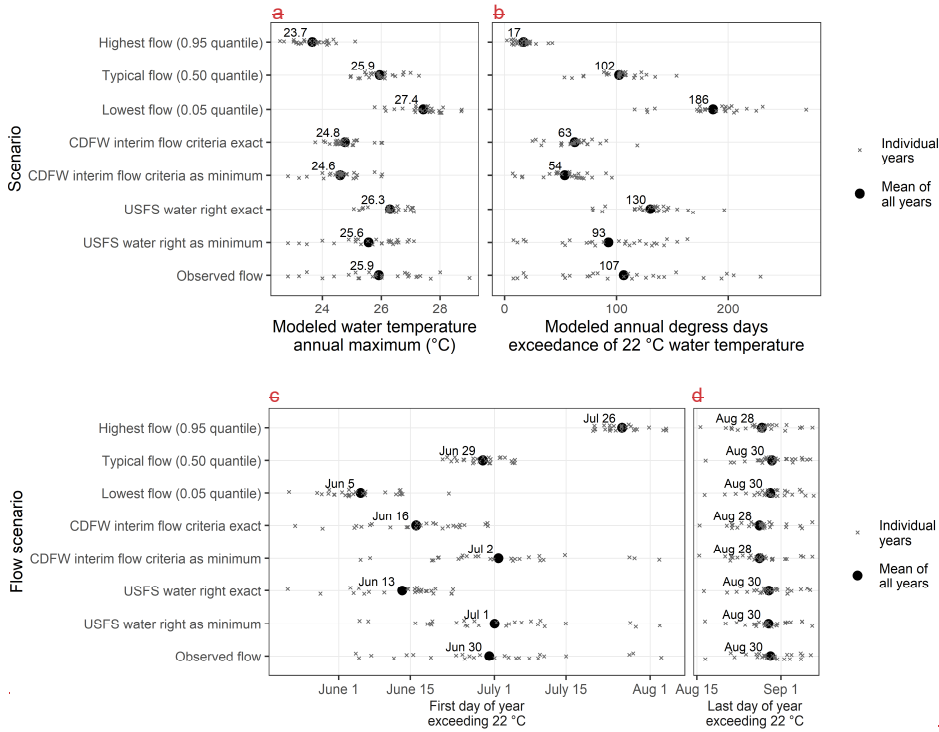


Figure 7.

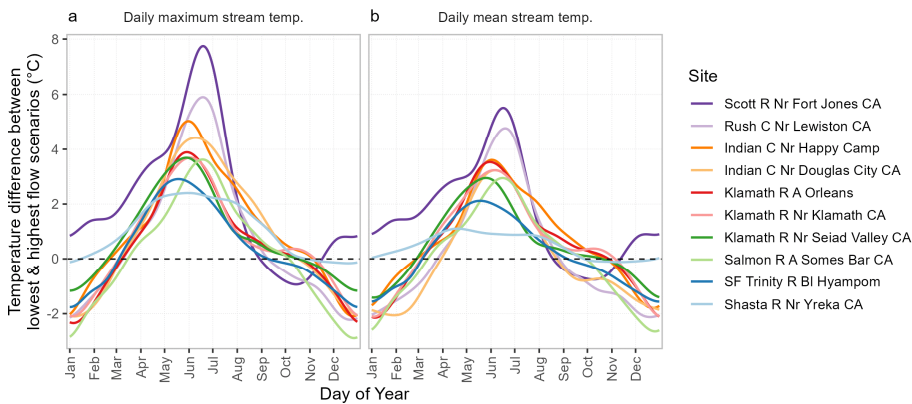
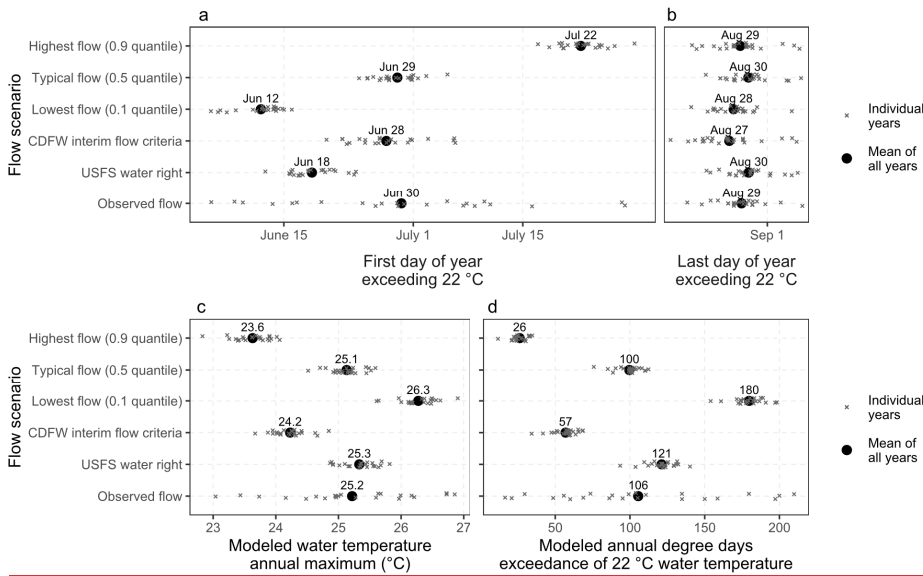


Figure 8. Modeled stream temperature differences between lowest flow (0.1 quantile) and highest flow (0.9 quantile) scenarios throughout the year for (a) T_{max} and (b) T_{mean} at 10 Klamath Basin sites estimated using GAM7.

803
804



805

806 **Figure 9.** (a) Annual maximum stream temperature, (b) annual degree-days exceeding 22 °C,
807 and (c) first day and (d) last day each year when DM_{xST} exceeds T_{max} exceeded 22 °C predicted
808 using a statistical in Scott River model scenarios pairing observed air temperatures for 1995–2020
809 with the same eight flow conditions scenarios. Means of all years are shown in Figure S8. Points
810 for with black points and grey “x” show individual years are, offset slightly for clarity. Data
811 labels are the mean of all years.

812

813

814 **5 Discussion**

815 Consistent with our hypothesis At all 10 sites, models with seasonally varying flow effects of
816 flows substantially outperformed models with a constant relationship between stream temperature
817 and flow. High flows have a strong cooling effect on stream temperatures in April–July, but less
818 influence during other months. The flexibility of GAMs, including non-linear and seasonally
819 varying relationships between stream temperature and flow, produced more accurate predictions
820 than harmonic regression models. Logistic regression of stream temperature with air
821 temperature, based Mohseni et al.’s (1998) popular method, indicating that the influence of flow
822 changes throughout the year. Models containing only air temperature performed particularly
823 poorly in comparison to the GAMs because it they did not include flow as a predictor. Our results
824 confirm previous findings that summer stream temperatures are negatively correlated with
825 covariate, while models with a linear effect of flow (Arora et al., had intermediate accuracy.

826 Flow had the strongest effect on water temperatures in April–July. The highest Scott River
827 management flow evaluated would substantially decrease exceedances of 22 °C and reduce
828 annual water temperature maximums. ~~2016; Isaak et al., 2017; Luce et al., 2014; Neumann et al.,~~
829 2003), and that flow more strongly affects DMxST than DMST (Asarian et al., 2020; Gu et al.,
830 1998; Gu and Li, 2002).

831 5.1 Model selection and the importance of seasonally varying and non-linear relationships

832 ~~After considering 13 models, we selected the GAM model with a two-day weighted air~~
833 ~~temperature (A_{2w}) whose slope varies by day of the year (D), a tensor product smooth of flow~~
834 ~~and day of the year (Q-D), and an A_{2w} -Q tensor product interaction (Table 1, Figure 4). We~~
835 ~~chose this model (GAM4 “tensors Q-D & A_{2w} -Q”) based on a combination of model fit (low~~
836 ~~RMSE, high R^2 , and low fREML score) and fewer effective degrees of freedom (edf) than other~~
837 ~~models with similar fit. This structure allowed modeled stream temperatures to respond flexibly~~
838 ~~to varying conditions in all three variables (D, A_{2w} , and Q). Although the three-way tensor~~
839 ~~GAM1 “tensor Q-D A_{2w} ” had the lowest fREML score, making it an appealing choice, it also~~
840 ~~had the highest edf, increasing the risk of being overfit. Indeed, when we experimented with~~
841 ~~applying GAM1 to model scenarios (not shown), the coolest air temperature scenarios (0.05~~
842 ~~quantile) had mid-July temperatures that were higher in the typical flow (0.50 quantile) than~~
843 ~~either the lowest flow (0.05 quantile) or highest flow (0.95 quantile) scenario, which seemed~~
844 ~~implausible.~~

845 ~~Comparing the relative performance of models with different smoothers and interactions~~
846 ~~provides insight into which are most important (Table 1, Figure 4, Figure S5). All models~~
847 ~~lacking seasonally varying flow effects (i.e., GAM8, GAM9, GAM10, GAM11, and Logistic13)~~
848 ~~performed worse than any model with seasonally varying flow effects, highlighting the~~
849 ~~importance of this feature. Modeled temperatures were biased high in April–June in models~~
850 ~~without seasonally varying flow effects, an issue that is diminished but still present in the~~
851 ~~Harmonic12 model that represents seasonal effects as perfectly symmetrical sine waves, and~~
852 ~~completely absent in the models that represents seasonal effects as flexible GAM smoothers~~
853 ~~(Figure S6). Models with tensors (i.e., GAM1, GAM2, GAM3, GAM4, GAM5, GAM6) had~~
854 ~~better fit than models with seasonally varying but linear relationships (e.g., GAM7), though the~~
855 ~~difference was not as great as the difference between seasonally constant models and seasonally~~
856 ~~varying models. For example, relative to the GAM7 model which is seasonally varying but~~
857 ~~linear, the GAM8 model with non-linear but seasonally constant relationships had a RMSE 0.4~~
858 ~~°C lower (0.96 °C vs. 1.35 °C) for DMxST and 0.2 °C lower (0.88 °C vs. 1.08 °C) for DMST~~
859 ~~(Table 1). The selected model, GAM4, which has a fully non-linear tensor product smooth of D~~
860 ~~and Q, and a tensor product interaction of A_{2w} and Q, has improved (relative to GAM8) RMSE~~
861 ~~of 0.89 °C for DMxST and 0.80 °C DMST and improved rREML scores (Table 1). In addition,~~
862 ~~the results for GAM3 (seasonally varying A_{2w} and Q-D tensor product smooth) and GAM5 (A_{2w} -~~
863 ~~D tensor product interaction and Q-D tensor product smooth), suggests that most of the~~
864 ~~improvement between GAM7 and GAM4 comes from the Q-D tensor product smooth rather~~
865 ~~than from the D-varying A_{2w} or Q- A_{2w} tensor product interaction (Table 1).~~

866 ~~The GAMs work well because they are able to represent the non-linear relationships and~~
867 ~~interactions between predictor variables present in our dataset. Heeding guidance from previous~~
868 ~~researchers we prevented overfitting by limiting the number of knots in the tensors (Jackson et~~
869 ~~al., 2018; Siegel and Volk, 2019). Our flexible approach takes maximal advantage of our multi-~~

870 decade daily calibration dataset featuring a range of environmental conditions (i.e., hot and cool
871 air temperatures and high and low flows) over the 4696 days. Our validation results suggest that
872 we have enough data to support our rather complex selected model GAM4. Future researchers
873 modeling temperatures at other sites may not have as much data, so should exercise caution and
874 may want to use the simpler GAM7 model.

875
876 5.3 Snow and groundwater mediate the effects of river flow—Model accuracy of our top model
877 and similar model structures were high for both T_{\max} and T_{mean} . For T_{mean} , our selected model's
878 LOYO CV RMSE ranged from 0.80–1.17 °C at 10 sites (Figure 5), better than the 0.75–1.75 °C
879 RMSE in Mohseni-based models at 14 sites within our study area (Manhard et al., 2018). In
880 addition to outperforming other models applied within our study area, our selected T_{mean} model
881 also had better LOYO CV RMSE than most single-station year-round daily statistical models
882 from around the world (all-site average model validation RMSE for each analysis's best
883 performing class of models: Ahmadi-Nedushan et al. [2007] 0.51 °C, Boudreault et al. [2019]
884 1.45 °C, Coleman et al. [2021] 1.3 °C, Koch and Grünewald [2010] 1.25 °C, Laanaya et al.
885 [2017] 1.44 °C, Letcher et al. [2016] 1.16 °C, Sohrabi et al. [2017] 1.25 °C, van Vliet et al.
886 [2011] 1.8 °C, and Soto et al. [2016] 1.20 °C). Our high model accuracy was achieved despite
887 using PRISM air temperatures instead of local measurements—favoring ease of replicability.

888 GAMs were a useful modeling approach because they represented the nonlinear relationships
889 and interactions between stream temperature and covariates. Our approach used >15-year
890 calibration datasets spanning environmental conditions (i.e., hot and cool air temperatures and
891 high and low flows). We prevented overfitting by restricting the number of knots in GAM
892 smoothers (Section 3.2), basing model selection on extrapolation tests that evaluate prediction
893 under expanded ranges of covariates (Section 3.3), and confirming that covariate responses and
894 interactions matched scientific hypotheses regarding underlying physical processes (Section 5.3).
895 Our selected model, GAM7, represented flow with two terms—a nonlinear smoother and a
896 partially nonlinear interaction between flow and day of year—whose combined effects (Figure 6)
897 provided enough flexibility for accurate predictions without overfitting. This two-term structure
898 incrementally improves upon previous methods for representing flow effects, with GAM7's
899 overall extrapolation CV RMSE 0.04 °C better than GAM6, the model with a simpler flow
900 effects structure nearly identical to Glover et al. (2020). Consistent with warnings from Siegel &
901 Volk (2019), tensors (fully nonlinear interactions) were too flexible and did not perform as well
902 as GAM7 when applied to conditions differing from the calibration dataset (i.e., extrapolation
903 tests), although tensor models still outperformed models without seasonally varying flow effects.

904 905 5.2 Magnitude and timing of flow effects on water temperature

906 Consistent with physical expectations, our results corroborate previous findings from northern
907 temperate rivers that during seasons when air temperatures are typically high and flows are
908 typically low (i.e., summer in our study area), lower flows are often temporally correlated with
909 higher stream temperatures (Arora et al., 2016; Isaak et al., 2017; Luce et al., 2014; Neumann et
910 al., 2003), and flow more strongly affects T_{\max} than T_{mean} (Asarian et al., 2020; Gu and Li, 2002;
911 Gu et al., 1998; Gu and Li, 2002). In our study streams, high flows had a strong cooling effect on
912 stream temperatures in April–July, but less influence during other months. Multiple linear

913 regression (MLR) models using monthly flow and air temperature at 239 Northwestern USA
914 sites not regulated by dams (Isaak et al., 2018) and spatial stream network models for eight
915 regions of the Western USA (FitzGerald et al., 2021) showed monthly timing and direction of
916 flow effects on stream temperatures (Figures S9–S10) similar to our results (Figure 8b), with the
917 exception of similar cooling in April and August whereas our models show weaker cooling in
918 August than in April. Monthly MLR modeling in 17 sites in Canada’s Frasier River Basin found
919 flow-mediated cooling effects on summer water temperatures were stronger in July than August
920 and weakest in September (Islam et al., 2019). In Poland, where inter-season flow differences are
921 less pronounced than in our study area, high flows were correlated with cooler water
922 temperatures in April–September, with the strongest relationships occurring in July–September
923 at mountainous snowmelt-fed rivers (Wrzesiński and Graf, 2022). An Eastern USA river study
924 using a daily year-round GAM found that water temperature decreased with increased flow from
925 April through mid-October (Yang & Moyer, 2020). Previous studies evaluating year-round
926 changes in the relationship between stream temperature and flow generally used monthly time
927 steps. Our daily model provides a more nuanced understanding of seasonal dynamics by
928 allowing this relationship to change smoothly at sub-monthly time scales, facilitating
929 identification of changes within a month, as well as the rate of change.

930 Flow-induced cooling in snowmelt-dominated rivers is common. Process-based modeling of a
931 Sierra Nevada river indicated early summer stream temperatures up to 16 °C cooler in a record
932 wet year relative to a dry year (Null et al., 2013). In steep Alaskan streams, average summer
933 stream temperatures were 3–5 °C cooler in high-snowpack years than low-snowpack years (Cline
934 et al., 2021). In the conterminous USA, including flow as a covariate improved daily stream
935 temperature predictions over air temperature only models in April–August, but only in
936 snowmelt-dominated streams (Sohrabi et al., 2017). Stronger flow effects occurred in inland
937 regions than coastal regions of the Western USA (Figure S10) (FitzGerald et al., 2021),
938 consistent with a greater percent of precipitation falling as snow (Klos et al., 2014). Climate
939 change studies have not parsed the separate influences of hydrology and air temperature on
940 stream temperature, but in snowmelt-dominated areas of western North America, predictions for
941 disproportionate spring and summer stream temperature warming are nearly ubiquitous and
942 attributed to snowpack declines causing lower flows in those seasons (Caldwell et al., 2013;
943 Crozier et al., 2020; Ficklin et al., 2014; Leach & Moore, 2019; Lee et al., 2020; Luo et al., 2013;
944 Null et al., 2013).

946 5.3 Model correspondence to physical mechanisms

947 We used air temperature and flow as the major predictors in our model, recognizing that these
948 predictors represent many processes that collectively determine stream temperatures. Air
949 temperature is not the most important component of stream heat budgets (Johnson, 2004;
950 Dugdale et al., 2017), but it has high predictive power because it is correlated with net radiative
951 flux, a key driver of stream heat budgets (Caissie 2006). Air temperature data resulted in high
952 model accuracy in our study, and are widely attainable unlike radiative fluxes.

953 The effects of flow on stream temperature vary throughout the year in response to the physical
954 mechanisms affecting stream energy balances. High flows speed downstream transit of water and
955 provide increased thermal mass that resists heating (or cooling). While flow has strong effects on
956 water temperature in April–July in our study area, its effects are substantially weaker—though

957 still present—in August. High flow can exert a dominant influence on water temperature, but this
958 influence wanes as flow recedes, leading to progressively greater influence of solar radiation and
959 air temperature. The relationship between flow and water temperature in our top-performing
960 model is nonlinear and varies with day. Marginal effects of decreasing flow diminish as flow
961 approaches 0 m³/s (Figure 6). At Scott River, August flows were much lower than July (Figure 2,
962 Figure 6), and by 15 August were always below 2.6 m³/s (92 ft³/s). These low August flows have
963 shallow water depth, low thermal mass, and slow transit times resulting in residence time
964 sufficient for water to heat up to equilibrium temperature (Bogan et al., 2003; Nichols et al.,
965 2014; Tague et al., 2007). During hot, dry conditions such occurs in our study area during
966 summer, evaporative cooling limits how high stream temperatures can rise even when flows are
967 extremely low (Mohseni & Stefan, 1999; Mohseni et al., 1998; Shaw et al., 2017). Flow
968 magnitude and seasonality at our study site is Wildfire smoke could also reduce warming of
969 August stream temperatures (David et al., 2018). Widespread fire is more likely during drought
970 conditions (Westerling, 2016), suggesting potential for smoke to confound low flow effects on
971 temperature by decreasing solar radiation. We did not include smoke in our models because the
972 data are difficult to process and we wanted easily replicable methods, but smoke effects on
973 stream temperatures peaked in August in our study area (Asarian et al., 2020). With less solar
974 radiation and cooler air temperatures than earlier months, T_{max} is almost always less than 22 °C
975 at Scott River by early September regardless of flow (Figure 7). In October–November, a period
976 of hydrologic transition when precipitation ends seasonal baseflow recession, flows had little
977 influence over stream temperature (Figure 8), but Scott River and two other sites had weak,
978 modal flow-temperature relationships (i.e., highest water temperatures at moderate flows) (Text
979 S5).

980 Groundwater contributes to the relationship between flow and stream temperature at our Scott
981 River site, as it does in many ~~driven by a mix of valley groundwater dynamics and snowmelt-~~
982 ~~driven mountain runoff (Foglia et al., 2013; Van Kirk and Naman, 2008). Groundwater~~
983 ~~contributes to the relationship between flow and stream temperature at our study site, as it does~~
984 ~~in many other rivers (Briggs et al., 2018; Isaak et al., 2017; Kelleher et al., 2012; Mayer, 2012;~~
985 ~~Nichols et al., 2014; Isaak et al., 2017). Thermal infrared imagery, field measurements~~
986 ~~(NCRWQCB, 2005), and a groundwater model (Tolley et al., 2019) confirm that the 10 km of~~
987 ~~river directly upstream of our study site are a gaining reach where valley constriction forces~~
988 ~~substantial groundwater into the Scott River, a common phenomenon at the outlet of alluvial~~
989 ~~valleys (Stanford and Ward, 1992). Scott River flows are driven by a mix of valley groundwater~~
990 ~~dynamics and snowmelt-driven mountain runoff (Foglia et al., 2013; Van Kirk and Naman,~~
991 ~~2008). 2019) all confirm that substantial groundwater is forced into the Scott River where the~~
992 ~~valley constricts upstream of our site, a common phenomenon at the outlet of alluvial valleys~~
993 ~~(Stanford and Ward, 1992). Process-based model scenarios predicted a doubling of groundwater-~~
994 ~~derived flow would cool peak summer Scott River temperatures. As mountain runoff recedes and~~
995 ~~tributaries are almost fully diverted for irrigation, the relative contribution of groundwater to~~
996 ~~surface flow at the valley outlet increases over the summer and becomes dominant (NCRWQCB,~~
997 ~~2005). Sediments underlying the river and its tributaries have high hydraulic conductivity, so~~
998 ~~groundwater and surface water are strongly connected (Tolley et al., 2019). During the May–~~
999 ~~September recession period when temperatures are of greatest biological concern, flows are~~
1000 ~~related to aquifer levels, and the relative proportions of valley outlet flow derived from mountain~~
1001 ~~runoff and groundwater are well-predicted by flow and day of year. Thus, even though these two~~
1002 ~~sources have different temperatures and our model does not explicitly differentiate them, the~~

1003 model performs well because the interaction of flow and day of year implicitly characterizes
1004 these dynamics adequately. Scenarios from a short-term process-based surface water model
1005 predicted doubling groundwater-derived flow would cool 30 July 2003 Scott River T_{max} by 2 °C,
1006 and a 50% reduction of groundwater-derived flow would warm temperatures by 2 °C
1007 (NCRWQCB, 2005). For comparison, applying our model to scenarios doubling or halving the
1008 3.03 m³/s (107 ft³/s) gaged flow for that same date predicts T_{max} 1.0 °C cooler or 0.7 °C warmer,
1009 respectively.

1010 The timing and magnitude of flow-induced cooling indicated by our models are similar to other
1011 snowmelt-dominated rivers. A process-based model of a Sierra Nevada river indicated early
1012 summer stream temperatures up to 16 °C cooler in an extreme wet year relative to a dry year
1013 (Null et al., 2013). Relative to a statistical model with only air temperature, including flow as a
1014 predictor improved stream temperature predictions in April through August in Idaho streams
1015 (Sohrabi et al. 2017). Most studies predicting climate change effects do not parse the separate
1016 contributions of hydrology and air temperature on stream temperature, but in snow-dominated
1017 areas of the western North America, predictions of disproportionate stream temperature warming
1018 expected in the summer and/or spring are nearly ubiquitous and attributed to earlier runoff timing
1019 from declining snowpack (Caldwell et al., 2017). Statistical models typically require many fewer
1020 variables as data inputs than process-based models do, so are often much simpler to develop
1021 (Caissie, 2006; Ouellet et al., 2020); however, this ease has tradeoffs. For example, our model
1022 does not differentiate between specific sources of inflows, which may have quite different
1023 temperature influences, nor how alternative management scenarios would spatially and
1024 temporally alter those inflows. If fundamental characteristics of valley hydrology (i.e.,
1025 management or climate) changed dramatically, model accuracy could suffer. Similarly, applying
1026 the model to covariate combinations beyond those used in calibration will degrade predictive
1027 accuracy (Section 5.5). To avoid overly complex models that overfit calibration data, we used
1028 extrapolation tests to favor selection of simpler more generalizable models. Our model does not
1029 incorporate longer-term (e.g., annual to decadal) variation in air temperature that affects
1030 groundwater temperatures and precipitation phase (e.g., snow or rain), so may underestimate
1031 responses relative to predictions from integrated process-based models (Leach & Moore 2019).
1032 2013; Crozier et al., 2020; Ficklin et al., 2014; Lee et al., 2020; Leach and Moore, 2019; Luo et
1033 al., 2013; Null et al., 2013).

1034 1035 5.4 Biological implications

1036 The prolonged snowmelt-driven flow recession in high-flow years keeps higher Scott River
1037 temperatures cooler longer into the summer than in low-flow years, extending flows extend the
1038 period when cool water habitat is available for fish (i.e., temperatures less than 22 °C) (Figure
1039 7). These cooler water temperatures give juvenile salmonids additional time to migrate
1040 downstream and reduce overall thermal stress for fish that rear in the Scott River through the
1041 entire summer. Climate change will likely continue to reduce snowpack and summer flows
1042 (Persad et al., 2020), increasing duration of detrimentally warm temperatures. Mean diel range in
1043 June–August exceeds 5 °C, providing hours every day when daily with temperatures are less than
1044 ≤22 °C even if T_{max} exceeds 22 °C. Salmonids can potentially persist by using
1045 thermal refugia where cool tributaries, groundwater, or hyporheic flow enters the river during the
1046 hotter parts of the day hours and then moving into forage in the mainstem to feed when

047 temperatures are cooler ([Brewitt & Danner, 2014](#); Sutton et al., 2007; Sutton ~~and~~ & Soto, 2012;
048 [Brewitt and Danner, 2014](#)). However, substantial portions of the Scott River and tributaries lack
049 surface flow during summer, especially in dry years, reducing [habitat](#) connectivity ~~between~~
050 ~~thermal refugia and mainstem habitats~~.

052 5.5 [Applications and](#) management implications

053 These models can be used not only to identify the seasonally varying influence of flow, but also
054 to predict future stream flow temperatures based on managed flow recommendations: ~~and to impute~~
055 ~~missing data~~. Instream flow management frameworks are evolving (Mierau et al., 2017; Poff et
056 al., 2017; Yarnell et al., 2020) and accurate stream temperature models provide a valuable tool
057 ~~for use in those processes to predict management outcomes~~.

058 Our modeling approach ~~is relatively easy to implement, especially in comparison to a process-~~
059 ~~based models, which we hope will could~~ facilitate water managers' ability to include stream
060 temperature as a management target: ~~in areas that do not currently have operational process-~~
061 ~~based models~~. For example, Siskiyou County is ~~currently~~ developing a groundwater
062 sustainability plan for [the](#) Scott Valley (Foglia et al., 2018). The current groundwater model
063 ([Tolley et al., 2019](#)) does not simulate water temperatures ([Tolley et al., 2019](#)), ~~so our~~
064 ~~temperature~~ Our model ~~could~~ [can](#) be used to ~~assess the predict~~ effects of ~~groundwater~~
065 ~~management on groundwater dependent ecosystems~~. Our results quantify the effect of flow on
066 ~~stream~~ [Scott River](#) temperatures, including the CDFW and USFS flow thresholds under
067 consideration, and could inform state agencies' development of new flow objectives. The CDFW
068 and USFS flows ~~are were~~ both predicted to ~~improve (i.e., cool) summer maximum annual~~
069 temperatures relative to current conditions, but improvements would be greater with the higher
070 CDFW flows: ([Figure 9](#)). We caution that while the CDFW and USFS flows are ~~relatively high~~
071 ~~compared to higher than typical~~ observed flows in late summer and early fall, for March to early
072 June they represent extreme drought conditions ([Figure 2b](#)), which has two implications. First, in
073 ~~dry years temperatures reach 22 °C in early or mid June in the observed flow scenario, which is~~
074 ~~only delayed in a small number of years in the scenarios with CDFW and USFS flows as~~
075 ~~minimums~~. Second, if river flows were diverted down to the CDFW and USFS flows in May and
076 June, then the 22 °C threshold would be reached an average of approximately two weeks earlier
077 ~~than occurred with the observed flows (Figure 7e), that could cause earlier exceedances of 22 °C~~
078 ([Figure 2b](#)). Surface water diversions for in lieu recharge (switching irrigation source from
079 groundwater to surface water) or managed aquifer recharge (Dahlke et al., 2018; Foglia et al.,
080 2013) should not use the CDFW and USFS flows to guide maximum diversion rates, but instead
081 be tailored to reduce deleterious effects on instream habitat including temperatures, such as
082 ceasing ~~diversions~~ by 1 June, the first date when measured ([Figure 2](#)) and modeled temperatures
083 ([Figure 7e](#)) reach 22 °C.

084 As with any ~~regression statistical~~ model, prediction accuracy ~~is likely to will~~ degrade when
085 applied to conditions more extreme than those present in the calibration dataset. ~~Our selected~~
086 ~~model interacts day of year with flow and air temperature, so extrapolation caution applies not~~
087 ~~just to the range of individual variables but also their combined distributions~~. Our calibration
088 dataset includes a wide range of hydrologic conditions, but no years without surface water
089 diversions or groundwater pumping because those activities occur every year. ~~Groundwater~~
090 ~~modeling efforts suggest that s~~Streamflow depletion from groundwater pumping ~~would be is~~

greater in dry years than wet years, ~~because in dry years pumping starts earlier, cumulative amounts pumped are greater, and the aquifer is drawn down lower~~ (Foglia et al., 2013; ~~Tolley et al., 2019~~). Simulated total valley-wide streamflow depletion peaks around 150,000 m³d⁻¹ (60 ft³/secs) in July ~~and~~ August (Foglia et al., 2013), exceeding streamflow in dry years. Our model should be suitable for modeling ~~stream temperatures in~~ dry years for scenarios with reduced pumping and/or diversions, which would presumably have flows similar to existing wet years (and hence are within the range of calibration flows); however, in wet years such scenarios would likely exceed the range of calibration flows and therefore be subject to ~~eonsiderably higher levels of~~ more uncertainty. ~~Any~~ Future application ~~of our model~~ to scenarios with flows higher than observed should be ~~done carefully and~~ interpreted with appropriate caveats.

Flow records are typically less available than water temperature records, so may constrain where our modeling approach can be applied. However, if site-specific flows were not available, data from a nearby site could be used if they were likely to be highly correlated (i.e., similar watershed characteristics). We did not systematically explore that issue, but the one site (South Fork Trinity River) where we used flows from an upstream station had prediction accuracy similar to the other nine sites (Figure 5). In addition, although our modeling approach should work well with records shorter than the >15-year datasets we used, we recommend further research to determine the minimum required period of record.

These models can also be used to fill gaps in stream temperature data records needed for other analyses (Glover et al., 2020). Their high accuracy suggests they would compare well with imputation methods used in recent daily year-round stream temperature analyses (Isaak et al., 2020; Johnson et al., 2021).

6 Conclusions

Statistical models indicate ~~Long-term daily stream temperature datasets enabled development of generalized additive models (GAMs) that include nonlinear and seasonally varying effects of flow and air temperature on stream temperature. Cross-validation indicated these models had higher accuracy than models that did not account for seasonally variable effects of flow, providing evidence that flow is important in controlling stream temperatures and that the influence of flow is variable through time. Results from these models indicated that high river flow has had a strong cooling effect on river temperatures during April through July in California's Scott River, at 10 sites in the Klamath Basin of California, corroborating similar to previous findings from process-based models in many snow-dominated rivers in western North America. A 24-year dataset of daily streams temperatures allowed us to develop a generalized additive model using tensor product smooths and interactions~~

Results from extrapolation cross-validation tests show that our selected model is robust in estimating stream temperatures under environmental conditions moderately outside of the range of conditions used to train the model (although see cautions in Section 5.5). We applied the model to instream flow management scenarios proposed by regulatory agencies at our focal study site, the Scott River, finding that these scenarios would improve stream temperatures. Relative to represent the non-linear and seasonally varying effects of flow and air temperature on stream temperature. Our model also includes the correlation structures inherent in the data, namely daily temporal autocorrelation historic conditions, the higher instream flow scenario

134 would reduce annual maximum temperature from 25.2 °C to 24.1 °C, reduce annual exceedances
135 of 22 °C (a cumulative thermal stress metric) from 106 to 51 degree-days, and random effects for
136 annual variation. Validation indicated excellent model performance, with average errors ≤ 1 °C.
137 This project contributes delay onset of water temperatures > 22 °C during some drought years.

138 These models contribute to an emerging body of work demonstrating the benefits use of
139 generalized additive models (GAMs) for modeling predicting daily river temperatures. Given the
140 flexibility of GAMs, there is a risk of overfitting data, but this risk can be minimized by
141 restricting the number of knots in GAM smoothers, confirming that smoother shape matches
142 scientific hypotheses regarding the underlying physical processes. Our models are easy to
143 implement and considering whether sample size is adequate for the complexity of the
144 model improve prediction accuracy of stream temperature responses to flow changes over models
145 without seasonally variable effects of flow, providing tools that managers can use to select flow
146 solutions most likely to protect species and ecosystems. The models are implemented in the R
147 software environment with publicly accessible code. Testing at 10 streams in our study region
148 indicated that models with seasonally variable flow effects had high prediction accuracy across
149 all streams, suggesting that these models have broad applicability over a range of stream types.
150 Our selected model, GAM7, incrementally improves upon previous methods for representing
151 flow effects. Model applications include those explored here (i.e., scenario prediction and
152 identifying periods of flow importance), as well as filling gaps in temperature time series. We
153 suggest that GAM7, as well as similar model structures (i.e., GAM6, GAM8) will perform well
154 across a range of streams. Model validation procedures, including extrapolation-based methods
155 when models are applied to new data, should be conducted to test model accuracy at new sites
156 and for datasets of variable periods of record.

157 These models identify the specific periods of the year when flow has greatest influence on
158 stream temperatures, and can be used to evaluate the thermal effects of alternative flow
159 management scenarios and prescriptions. The models are implemented in the R software
160 environment with publicly accessible code, and could be applied to model year-round daily
161 temperature in any stream with long-term measurements of flow and water temperature,
162 provided that air temperatures are available from a nearby weather station.

1164 **CRedit authorship contribution statement**

165 J. ~~Eli Asarian~~:E.A.: Conceptualization, Data curation, Methodology, Formal analysis,
166 Visualization, Writing – original draft, Writing – review & editing. ~~Crystal Robinson~~:C.R.:
167 Conceptualization, Investigation, Data curation, Funding acquisition, Project administration,
168 Writing - review & editing. L.G.: Writing - review & editing.

1170 **Acknowledgments**

1171 The Klamath Tribal Water Quality Consortium (Karuk Tribe, Yurok Tribe, Hoopa Valley Tribe,
1172 Quartz Valley Indian Reservation, and Resighini Rancheria) supported Eli AsarianJ.E.A. and
1173 L.G., using funds provided by the U.S. Environmental Protection Agency, Region 9. Maija
1174 Meneks (KNF) and Callie McConnell (USFS Corvallis) provided the USFS water temperature
1175 data. Isaiah Williams, Alex Case, Sean Ryan and Marla Bennett (QVIR) assisted with data

176 collection. [Edward Jones \(USGS\) provided code for non-linear regression.](#) [Laurel Genzoli](#)
177 [reviewed a draft of Taylor Daley \(USFWS Arcata\) provided USFWS water temperature data.](#)
178 [Daniel Isaak and Sara John provided data from Isaak et al. \(2018\) and FitzGerald et al. \(2021\),](#)
179 [respectively. WRR editors and reviewers provided comments that substantially improved this](#)
1180 [manuscript.](#)

1182 Data Availability Statement

1183 All [input and output](#) data and [eodecodes](#) are archived in the online repository HydroShare
1184 ([Asarian and Robinson, 2021 et al., 2022,](#)
1185 <http://www.hydroshare.org/resource/a6653e2919964f9b840ec0340d86e11c>). USBR [and USGS](#)
1186 [stream temperature data \(Smith et al., 2018\)](#) are also available at: [https://or.water.usgs.gov/cgi-](https://or.water.usgs.gov/cgi-bin/grapher/graph_setup.pl?basin_id=all&site_id=11519500-)
1187 https://cdec.water.ca.gov/dynamicapp/staMeta?station_id=RCL. [CDWR stream temperature data](#)
1188 [are also available are available at](#)
1189 <https://wdl.water.ca.gov/WaterDataLibrary/StationDetails.aspx?Station=F3410000>. Gridded
1190 PRISM air temperature data (Daly et al., 2008) are also available at:
1191 <https://prism.oregonstate.edu/explorer/>. [GHCN-D air temperature data \(Menne et al., 2012a,](#)
1192 [2012b\)](#) are also available at <http://doi.org/10.7289/V5D21VHZ>.
1193

1195 References

- 1196 [Alger, M., Lane, B. A., & Neilson, B. T. \(2021\). Combined influences of irrigation diversions](#)
1197 [and associated subsurface return flows on river temperature in a semi-arid region. *Hydrological*](#)
1198 [Processes, 35\(8\), e14283. <https://doi.org/10.1002/hyp.14283>](#)
- 1199 Amodio, S., Aria, M., & D'Ambrosio, A. (2014). On concavity in nonlinear and nonparametric
1200 regression models. *Statistica*, 74(1), 85–98. <https://doi.org/10.6092/issn.1973-2201/4599>
- 1201 Arismendi, I., Safeeq, M., Dunham, J. B., & Johnson, S. L. (2014). Can air temperature be used
1202 to project influences of climate change on stream temperature? *Environmental Research Letters*,
1203 9(8), 084015. <https://doi.org/10.1088/1748-9326/9/8/084015>
- 1204 Arora, R., Tockner, K., & Venohr, M. (2016). Changing river temperatures in northern Germany:
1205 Trends and drivers of change. *Hydrological Processes*, 30(17), 3084–3096.
1206 <https://doi.org/10.1002/hyp.10849>
- 1207 Asarian, J.E., Cressey, L., Bennett, B., Grunbaum, J., Cyr, L., Soto, T., & Robinson, C. (2020).
1208 Influence of snowpack, streamflow, air temperature, and wildfire smoke on Klamath Basin
1209 stream temperatures, 1995-2017. Eureka, CA: Riverbend Sciences.
1210 <https://doi.org/10.13140/RG.2.2.22934.47681>
- 1211 [Asarian, J. E., & Robinson, C., & Genzoli, L. \(2022+\). Data and codes for: Modeling seasonal](#)
1212 [effects of river flow on water temperatures in an agriculturally dominated California river.](#)
1213 [HydroShare, <http://www.hydroshare.org/resource/a6653e2919964f9b840ec0340d86e11c>](#)

- 1214 Asarian, J. E., & Walker, J. D. (2016). Long-term trends in streamflow and precipitation in
1215 Northwest California and Southwest Oregon, 1953-2012. *Journal of the American Water*
1216 *Resources Association*, 52(1), 241–261. <https://doi.org/10.1111/1752-1688.12381>
- 1217 Baayen, R. H., van Rij, J., de Cat, C., & Wood, S. (2018). Autocorrelated errors in experimental
1218 data in the language sciences: some solutions offered by generalized additive mixed models. In
1219 D. Speelman, K. Heylen, & D. Geeraerts (Eds.), *Mixed-Effects Regression Models in Linguistics*
1220 (pp. 49–69). Springer International Publishing. https://doi.org/10.1007/978-3-319-69830-4_4
- 1221 Bartholow, J. M. (1991). A modeling assessment of the thermal regime for an urban sport
1222 fishery. *Environmental Management*, 15(6), 833. <https://doi.org/10.1007/BF02394821>
- 1223 Benyahya, L., Caissie, D., St-Hilaire, A., Ouarda, T. B. M. J., & Bobée, B. (2007a). A review of
1224 statistical water temperature models. *Canadian Water Resources Journal / Revue Canadienne*
1225 *Des Ressources Hydriques*, 32(3), 179–192. <https://doi.org/10.4296/cwrj3203179>
- 1226 Benyahya, L., St-Hilaire, A., Ouarda, T. B. M. J., Bobée, B., & Ahmadi-Nedushan, B. (2007b).
1227 Modeling of water temperatures based on stochastic approaches: Case study of the Deschutes
1228 River. *Journal of Environmental Engineering and Science*, 6(4), 437–448.
1229 <https://doi.org/10.1139/s06-067>
- 1230 Benyahya, L., St-Hilaire, A., Ouarda, T., Bobee, B., & Dumas, J. (2008). Comparison of non-
1231 parametric and parametric water temperature models on the Nivelle River, France. *Hydrological*
1232 *Sciences Journal*, 53(3), 640–655.
- 1233 ~~Bernhardt, E. S., Heffernan, J. B., Grimm, N. B., Stanley, E. H., Harvey, J., Bogan, T.,~~
1234 ~~Mohseni, W., Arroita, M., Appling, A. P., Cohen, M. J., McDowell, W. H., Hall, R. O., Read, J.~~
1235 ~~S., Roberts, B., & Stefan, H. J., Stets, E. G., & Yackulic, C. B. (2017). The metabolic regimes of~~
1236 ~~flowing waters: Metabolic regimes. *Limnology and Oceanography*.~~
1237 ~~<https://doi.org/10.1002/lno.10726>~~
- 1238 ~~Bodeker, G. (2003). Stream~~
1239 ~~vertical ozone and temperature profiles measured by ozonesondes at Lauder, New Zealand:~~
1240 ~~1986–1996. *Journal of Geophysical equilibrium temperature relationship. *Water Resources**~~
1241 ~~*Research-Atmospheres*, 103(D22), 28661–28681, 39(9), 1245.~~
1242 ~~<https://doi.org/10.1029/98JD02581-2003WR002034>~~
- 1243 Boudreault, J., Bergeron, N. E., St-Hilaire, A., & Chebana, F. (2019). Stream temperature
1244 modeling using functional regression models. *Journal of the American Water Resources*
1245 *Association*, 55(6), 1382–1400. <https://doi.org/10.1111/1752-1688.12778>
- 1246 Boyd, M., and Kasper, B. (2003). Analytical methods for dynamic open channel heat and mass
1247 transfer: Methodology for Heat Source model version 7.0. Portland, OR: Oregon Department of
1248 Environmental Quality.
- 1249 Brewitt, K. S., & Danner, E. M. (2014). Spatio-temporal temperature variation influences
1250 juvenile steelhead (*Oncorhynchus mykiss*) use of thermal refuges. *Ecosphere*, 5(7), art92.
1251 <https://doi.org/10.1890/ES14-00036.1>
- 1252 Briggs, M. A., Johnson, Z. C., Snyder, C. D., Hitt, N. P., Kurylyk, B. L., Lautz, L., Irvine, D. J.,
1253 Hurley, S. T., & Lane, J. W. (2018). Inferring watershed hydraulics and cold-water habitat
1254 persistence using multi-year air and stream temperature signals. *Science of The Total*
1255 *Environment*, 636, 1117–1127. <https://doi.org/10.1016/j.scitotenv.2018.04.344>

- 1256 Brown, G. W. (1969). Predicting temperatures of small streams. *Water Resources Research*,
1257 5(1), 68–75. <https://doi.org/10.1029/WR005i001p00068>
- 1258 Cade, B. S., & Noon, B. R. (2003). A gentle introduction to quantile regression for ecologists.
1259 *Frontiers in Ecology and the Environment*, 1(8), 412–420. [https://doi.org/10.1890/1540-](https://doi.org/10.1890/1540-9295(2003)001[0412:AGITQR]2.0.CO;2)
1260 [9295\(2003\)001\[0412:AGITQR\]2.0.CO;2](https://doi.org/10.1890/1540-9295(2003)001[0412:AGITQR]2.0.CO;2)
- 1261 Caissie, D. (2006). The thermal regime of rivers: A review. *Freshwater Biology*, 51(8), 1389–
1262 1406. <https://doi.org/10.1111/j.1365-2427.2006.01597.x>
- 1263 [Caissie, D., El-Jabi, N., & Satish, M. G. \(2001\). Modelling of maximum daily water
1264 temperatures in a small stream using air temperatures. *Journal of Hydrology*, 251\(1\), 14–28.
1265 \[https://doi.org/10.1016/S0022-1694\\(01\\)00427-9\]\(https://doi.org/10.1016/S0022-1694\(01\)00427-9\)](https://doi.org/10.1016/S0022-1694(01)00427-9)
- 1266 Caldwell, R. J., Gangopadhyay, S., Bountry, J., Lai, Y., & Elsner, M. M. (2013). Statistical
1267 modeling of daily and subdaily stream temperatures: Application to the Methow River Basin,
1268 Washington. *Water Resources Research*, 49(7), 4346–4361. <https://doi.org/10.1002/wrcr.20353>
- 1269 [CDFW \(California Department of Fish and Wildlife \(CDFW\)\) \(2017\). Interim Instream Flow
1270 Criteria for the Protection of Fishery Resources in the Scott River Watershed, Siskiyou County.
1271 \[https://web.archive.org/web/20210324204650if_/https://nrm.dfg.ca.gov/FileHandler.ashx?Docu
1272 mentID=143476\]\(https://web.archive.org/web/20210324204650if_/https://nrm.dfg.ca.gov/FileHandler.ashx?DocumentID=143476\).](https://web.archive.org/web/20210324204650if_/https://nrm.dfg.ca.gov/FileHandler.ashx?DocumentID=143476)
- 1273 Chandesris, A., Van Looy, K., Diamond, J. S., & Souchon, Y. (2019). Small dams alter thermal
1274 regimes of downstream water. *Hydrology and Earth System Sciences*, 23(11), 4509–4525.
1275 <https://doi.org/10.5194/hess-23-4509-2019>
- 1276 [Cline, T. J., Schindler, D. E., Walsworth, T. E., French, D. W., Cox, N. J. \(2006\). Speaking
1277 Stata: In Praise of Trigonometric Predictors. *The Stata Journal: Promoting Communications on
1278 Statistics and Stata*, 6\(4\), 561–579. <https://doi.org/10.1177/1536867X0600600408>](https://doi.org/10.1177/1536867X0600600408)
- 1279 [& Lisi, P. J. \(2020\). Low snowpack reduces thermal response diversity among streams across a
1280 landscape. *Limnology and Oceanography Letters*, 5\(3\), 254–263.
1281 <https://doi.org/10.1002/lo12.10148>.](https://doi.org/10.1002/lo12.10148)
- 1282 [Coleman, D., Bevitt, R., & Reinfelds, I. \(2021\). Predicting the thermal regime change of a
1283 regulated snowmelt river using a generalised additive model and analogue reference streams.
1284 *Environmental Processes*, 8\(2\), 511–531. <https://doi.org/10.1007/s40710-021-00501-7>](https://doi.org/10.1007/s40710-021-00501-7)
- 1285 Crozier, L. G., Siegel, J. E., Wiesebron, L. E., Trujillo, E. M., Burke, B. J., Sandford, B. P., &
1286 Widener, D. L. (2020). Snake River sockeye and Chinook salmon in a changing climate:
1287 Implications for upstream migration survival during recent extreme and future climates. *PLOS*
1288 *ONE*, 15(9), e0238886. <https://doi.org/10.1371/journal.pone.0238886>
- 1289 Dahlke, H., Brown, A., Orloff, S., Putnam, D., & O’Geen, T. (2018). Managed winter flooding
1290 of alfalfa recharges groundwater with minimal crop damage. *California Agriculture*, 72(1), 1–11.
1291 <https://doi.org/10.3733/ca.2018a0001>
- 1292 [Dahlke, F. T., Wohlrab, S., Butzin, M., & Pörtner, H.-O. \(2020\). Thermal bottlenecks in the life
1293 cycle define climate vulnerability of fish. *Science*, 369\(6499\), 65–70.
1294 <https://doi.org/10.1126/science.aaz3658>](https://doi.org/10.1126/science.aaz3658)
- 1295 Daly, C., Halbleib, M., Smith, J. I., Gibson, W. P., Doggett, M. K., Taylor, G. H., Curtis, J., &
1296 Pasteris, P. P. (2008). Physiographically sensitive mapping of climatological temperature and

- 1297 precipitation across the conterminous United States. *International Journal of Climatology*,
1298 28(15), 2031–2064. <https://doi.org/10.1002/joc.1688>
- 1299 David, A. T., Asarian, J. E., & Lake, F. K. (2018). Wildfire smoke cools summer river and
1300 stream water temperatures. *Water Resources Research*, 54(10), 7273–7290.
1301 <https://doi.org/10.1029/2018WR022964>
- 1302 Drake, D., Tate, K., & Carlson, H. (2000). Analysis shows climate-caused decreases in Scott
1303 River fall flows. *California Agriculture*, 54(6), 46–49. <https://doi.org/10.3733/ca.v054n06p46>
- 1304 Dugdale, S. J., Hannah, D. M., & Malcolm, I. A. (2017). River temperature modelling: A review
1305 of process-based approaches and future directions. *Earth-Science Reviews*, 175, 97–113.
1306 <https://doi.org/10.1016/j.earscirev.2017.10.009>
- 1307 Dugdale, S. J., Malcolm, I. A., Kantola, K., & Hannah, D. M. (2018). Stream temperature under
1308 contrasting riparian forest cover: Understanding thermal dynamics and heat exchange processes.
1309 *Science of The Total Environment*, 610–611, 1375–1389.
1310 <https://doi.org/10.1016/j.scitotenv.2017.08.198>
- 1311 ~~Dunham, J., Chandler, G., Rieman, B., Martin, D. (2005). Measuring stream temperature with~~
1312 ~~digital data loggers: A user's guide (USDA Forest Service Gen. Tech. Rep. RMRS-GTR-~~
1313 ~~150WWW). http://www.fs.fed.us/rm/pubs/rmrs_gtr150.pdf~~
- 1314 Dymond, J. R. (1984). Water temperature change caused by abstraction. *Journal of Hydraulic*
1315 *Engineering*, 110(7), 987–991. [https://doi.org/10.1061/\(ASCE\)0733-9429\(1984\)110:7\(987\)](https://doi.org/10.1061/(ASCE)0733-9429(1984)110:7(987))
- 1316 ~~Eriekson, T., Fasiolo, M., Wood, S. N., Zaffran, M., Nedellec, R., & Goude, Y. (2020). Fast~~
1317 ~~calibrated additive quantile regression. & Stefan, H.-G. (2000). Linear Air/Water Temperature~~
1318 ~~Correlations for Streams during Open Water Periods. *Journal of Hydrologic Engineering*, 5(3),~~
1319 ~~317–321. *the American Statistical Association*, 1–11. [https://doi.org/10.5194/hess-18-4897-2014](https://doi.org/10.1061/(ASCE)1084-
1320 0699(2000)5:3(317)1080/01621459.2020.1725521</p><p>1321 Ficklin, D. L., Barnhart, B. L., Knouft, J. H., Stewart, I. T., Maurer, E. P., Letsinger, S. L., &
1322 Whittaker, G. W. (2014). Climate change and stream temperature projections in the Columbia
1323 River basin: Habitat implications of spatial variation in hydrologic drivers. <i>Hydrology and Earth</i>
1324 <i>System Sciences</i>, 18(12), 4897–4912. <a href=)~~
- 1325 FitzGerald, A. M., John, S. N., Apgar, T. M., Mantua, N. J., & Martin, B. T. (2021). Quantifying
1326 thermal exposure for migratory riverine species: Phenology of Chinook salmon populations
1327 predicts thermal stress. *Global Change Biology*, 27(3), 536–549.
1328 <https://doi.org/10.1111/gcb.15450>
- 1329 Foglia, L., McNally, A., & Harter, T. (2013). Coupling a spatiotemporally distributed soil water
1330 budget with stream-depletion functions to inform stakeholder-driven management of
1331 groundwater-dependent ecosystems. *Water Resources Research*, 49(11), 7292–7310.
1332 <https://doi.org/10.1002/wrcr.20555>
- 1333 Foglia, L., Neumann, J., Tolley, D., Orloff, S., Snyder, R., & Harter, T. (2018). Modeling guides
1334 groundwater management in a basin with river–aquifer interactions. *California Agriculture*,
1335 72(1), 84–95. <https://doi.org/10.3733/ca.2018a0011>
- 1336 Folegot, S., Hannah, D. M., Dugdale, S. J., Kurz, M. J., Drummond, J. D., Klaar, M. J., Lee-
1337 Cullin, J., Keller, T., Martí, E., Zarnetske, J. P., Ward, A. S., & Krause, S. (2018). Low flow

- 1338 controls on stream thermal dynamics. *Limnologia*, 68, 157–167.
1339 <https://doi.org/10.1016/j.limno.2017.08.003>
- 1340 Fullerton, A. H., Torgersen, C. E., Lawler, J. J., Faux, R. N., Steel, E. A., Beechie, T. J.,
1341 Ebersole, J. L., & Leibowitz, S. G. (2015). Rethinking the longitudinal stream temperature
1342 paradigm: Region-wide comparison of thermal infrared imagery reveals unexpected complexity
1343 of river temperatures. *Hydrological Processes*, 29(22), 4719–4737.
1344 <https://doi.org/10.1002/hyp.10506>
- 1345 Gibeau, P., & Palen, W. J. (2020). Predicted effects of flow diversion by run-of-river
1346 hydropower on bypassed stream temperature and bioenergetics of salmonid fishes. *River*
1347 *Research and Applications*, 36(9), 1903–1915. <https://doi.org/10.1002/rra.3706>
- 1348 ~~Georges, B., Michez, A., Latte, N., Lejeune, P., & Brostaux, Y. (2021). Water stream heating~~
1349 ~~dynamics around extreme temperature events: An innovative method combining GAM and~~
1350 ~~differential equations. *Journal of Hydrology*, 601, 126600.~~
1351 ~~<https://doi.org/10.1016/j.jhydrol.2021.126600>~~
- 1352 ~~Glover, R. S., Gallie, A., Schaeffli-Soulsby, C., Fryer, R. J., Birkel, C., & Malcolm, I. A.~~
1353 ~~(2020). Quantifying the relative importance of stock level, river temperature and discharge on~~
1354 ~~the abundance of juvenile Atlantic salmon (*Salmo salar*). *Ecohydrology*, 13(6), e2231.~~
1355 ~~<https://doi.org/10.1002/eco.2231>~~
- 1356 ~~B., Lehning, M., Parlange, M. B., & Huwald, H. (2015). Stream temperature prediction in~~
1357 ~~ungauged basins: Review of recent approaches and description of a new physics-derived~~
1358 ~~statistical model. *Hydrol. Earth Syst. Sci.*, 19(9), 3727–3753. [https://doi.org/10.5194/hess-19-](https://doi.org/10.5194/hess-19-3727-2015)~~
1359 ~~[3727-2015](https://doi.org/10.5194/hess-19-3727-2015)~~
- 1360 Gu, R. R., & Li, Y. (2002). River temperature sensitivity to hydraulic and meteorological
1361 parameters. *Journal of Environmental Management*, 66(1), 43–56.
1362 <https://doi.org/10.1006/jema.2002.0565>
- 1363 Gu, R., Montgomery, S., & Austin, T. A. (1998). Quantifying the effects of stream discharge on
1364 summer river temperature. *Hydrological Sciences Journal*, 43(6), 885–904.
1365 <https://doi.org/10.1080/02626669809492185>
- 1366 ~~Hannah, D. M., Malcolm, I. A., & Bradley, C. (2009). Seasonal hyporheic temperature dynamics~~
1367 ~~over riffle bedforms. *Hydrological Processes*, 23(15), 2178–2194.~~
1368 ~~<https://doi.org/10.1002/hyp.7256>~~
- 1369 ~~Imholt, C., Gibbins, C. N., Malcolm, I. A., Langan, S., & Soulsby, C. (2010). Influence of~~
1370 ~~riparian cover on stream temperatures and the growth of the mayfly *Baetis rhodani* in an upland~~
1371 ~~stream. *Aquatic Ecology*, 44(4), 669–678. <https://doi.org/10.1007/s10452-009-9305-0>~~
- 1372 ~~Isaak, D. J., Luce, C. H., Horan, D. L., Chandler, G. L., Wollrab, S. P., Dubois, W. B., & Nagel,~~
1373 ~~D. E. (2020). Hamm, W. J., Rempe, D. M., Dralle, D. N., Dawson, T. E., Lovill, S Thermal~~
1374 ~~regimes of perennial rivers and streams in the Western United States. *Journal of the American*~~
1375 ~~*Water Resources Association*, 1752-1688.12864. <https://doi.org/10.1111/1752-1688.12864>~~
- 1376 ~~M., Bryk, A. B., Bish, D. L., Schieber, J., & Dietrich, W. E. (2019). Lithologically Controlled~~
1377 ~~Subsurface Critical Zone Thickness and Water Storage Capacity Determine Regional Plant~~
1378 ~~Community Composition. *Water Resources Research*, 55(4), 3028–3055.~~
1379 ~~<https://doi.org/10.1029/2018WR023760>~~

- 380 [Helsel, D. R., Hirsch, R. M., Ryberg, K. R., Archfield, S. A., & Gilroy, E. J. \(2020\). Statistical](#)
381 [methods in water resources \(U.S. Geological Survey Techniques and Methods, book 4, chapter](#)
382 [A3\). https://doi.org/10.3133/tm4A3](#)
- 383 [Hilderbrand, R. H., Kashiwagi, M. T., & Prochaska, A. P. \(2014\). Regional and Local Scale](#)
384 [Modeling of Stream Temperatures and Spatio-Temporal Variation in Thermal Sensitivities.](#)
385 [Environmental Management, 54\(1\), 14–22. https://doi.org/10.1007/s00267-014-0272-4](#)
- 1386 Isaak, D. J., Luce, C. H., Horan, D. L., Chandler, G. L., Wollrab, S. P., & Nagel, D. E. (2018).
1387 Global warming of salmon and trout rivers in the Northwestern U.S.: Road to ruin or path
1388 through purgatory? *Transactions of the American Fisheries Society*, 147(3), 566–587.
1389 <https://doi.org/10.1002/tafs.10059>
- 1390 Isaak, D. J., Wenger, S. J., Peterson, E. E., Hoef, J. M. V., Nagel, D. E., Luce, C. H., Hostetler,
1391 S. W., Dunham, J. B., Roper, B. B., Wollrab, S. P., Chandler, G. L., Horan, D. L., & Parkes-
1392 Payne, S. (2017). The NorWeST summer stream temperature model and scenarios for the
1393 Western U.S.: A crowd-sourced database and new geospatial tools foster a user community and
1394 predict broad climate warming of rivers and streams. *Water Resources Research*, 53(11), 9181–
1395 9205. <https://doi.org/10.1002/2017WR020969>
- 396 [Islam, S. U., Hay, R. W., Déry, S. J., & Booth, B. P. \(2019\). Modelling the impacts of climate](#)
397 [change on riverine thermal regimes in western Canada's largest Pacific watershed. *Scientific*](#)
398 [Reports, 9, 11398. https://doi.org/10.1038/s41598-019-47804-2](#)
- 1399 Jackson, F. L., Fryer, R. J., Hannah, D. M., Millar, C. P., & Malcolm, I. A. (2018). A spatio-
1400 temporal statistical model of maximum daily river temperatures to inform the management of
1401 Scotland's Atlantic salmon rivers under climate change. *Science of The Total Environment*, 612,
1402 1543–1558. <https://doi.org/10.1016/j.scitotenv.2017.09.010>
- 1403 Johnson, S. L. (2004). Factors influencing stream temperatures in small streams: Substrate
1404 effects and a shading experiment. *Canadian Journal of Fisheries and Aquatic Sciences*, 61(6),
1405 913–923.
- 406 [Johnson, Z. C., Johnson, B. G., Briggs, M. A., ~~Devine, W. D.~~, Snyder, C. D., Hitt, N. P., ~~Hare,~~](#)
407 [D. K., & Minkova, T. V. \(2020\). Paired air water & ~~Devine, W. D. \(2021\). Heed the data gap:~~](#)
408 [Guidelines for using incomplete datasets in annual stream temperature patterns reveal](#)
409 [hydrogeological controls on stream thermal regimes at watershed to continental scales. *Journal*](#)
410 [of Hydrology, 587, 124929. analyses. Ecological Indicators, 122, 107229.](#)
411 <https://doi.org/10.1016/j.jhydrol.2020.124929>
<https://doi.org/10.1016/j.jhydrol.2020.124929>
- 412 [Jones, E. C., Perry, R. W., Risley, J. C., Som, N. A., & Hetrick, N. J. \(2016\). Construction,](#)
413 [calibration, and validation of the RBM10 water temperature model for the Trinity River,](#)
414 [Northern California \(U.S. Geological Survey Open-File Report 2016-1056\).](#)
415 <https://doi.org/10.3133/ofr20161056>
- 1416 Kelleher, C., Wagener, T., Gooseff, M., McGlynn, B., McGuire, K., & Marshall, L. (2012).
1417 Investigating controls on the thermal sensitivity of Pennsylvania streams. *Hydrological*
1418 *Processes*, 26(5), 771–785. <https://doi.org/10.1002/hyp.8186>
- 1419 Kim, J.-S., & Jain, S. (2010). High-resolution streamflow trend analysis applicable to annual
1420 decision calendars: A western United States case study. *Climatic Change*, 102(3–4), 699–707.
1421 <https://doi.org/10.1007/s10584-010-9933-3>

- 1422 ~~KNF (Klamath National Forest-(KNF,-)) (2010-).~~ Klamath National Forest Sediment and
1423 Temperature Monitoring Plan and Quality Assurance Project Plan. Yreka, CA: Klamath National
1424 Forest.
1425 [https://web.archive.org/web/http://www.waterboards.ca.gov/water_issues/programs/tmdl/records](https://web.archive.org/web/http://www.waterboards.ca.gov/water_issues/programs/tmdl/records/region_1/2013/ref4082.pdf)
1426 [/region_1/2013/ref4082.pdf](https://web.archive.org/web/http://www.waterboards.ca.gov/water_issues/programs/tmdl/records/region_1/2013/ref4082.pdf).
- 1427 ~~KNF (Klamath National Forest) (2011).~~ Klamath National Forest, Water and Air Temperature
1428 Monitoring Protocol, May 2011. Yreka, CA: Klamath National Forest.
- 1429 ~~Klemeš, V. (1986).~~ Operational testing of hydrological simulation models. *Hydrological*
1430 *Sciences Journal*, 31(1), 13–24. <https://doi.org/10.1080/02626668609491024>
- 1431 ~~Klos, P. Z., Link, T. E., & Abatzoglou, J. T. (2014).~~ Extent of the rain-snow transition zone in
1432 the western U.S. under historic and projected climate. *Geophysical Research Letters*, 41(13),
1433 4560–4568. <https://doi.org/10.1002/2014GL060500>
- 1434 Koch, H., & Grünewald, U. (2010). Regression models for daily stream temperature simulation:
1435 Case studies for the river Elbe, Germany. *Hydrological Processes*, 24(26), 3826–3836.
1436 <https://doi.org/10.1002/hyp.7814>
- 1437 ~~Kurylyk, B. L., MacQuarrie, K. T. B., Kothandaraman, V. (1971).~~ Analysis of Water
1438 Temperature Variations in Large River. *Journal of the Sanitary Engineering Division*, 97(1), 19–
1439 31. <https://doi.org/10.1061/JSEDAI.0001242>
- 1440 ~~Linnansaari, T., Cunjak, R. A., & Curry, R. A. (2015).~~ Preserving, augmenting, and creating
1441 cold-water thermal refugia in rivers: Concepts derived from research on the Miramichi River,
1442 New Brunswick (Canada). *Ecohydrology*, 8(6), 1095–1108. <https://doi.org/10.1002/eco.1566>
- 1443 Laanaya, F., St-Hilaire, A., & Gloaguen, E. (2017). Water temperature modelling: Comparison
1444 between the generalized additive model, logistic, residuals regression and linear regression
1445 models. *Hydrological Sciences Journal*, 62(7), 1078–1093.
1446 <https://doi.org/10.1080/02626667.2016.1246799>
- 1447 Leach, J. A., & Moore, R. D. (2019). Empirical stream thermal sensitivities may underestimate
1448 stream temperature response to climate warming. *Water Resources Research*, 55(7), 5453–5467.
1449 <https://doi.org/10.1029/2018WR024236>
- 1450 Lee, S.-Y., Fullerton, A. H., Sun, N., & Torgersen, C. E. (2020). Projecting spatiotemporally
1451 explicit effects of climate change on stream temperature: A model comparison and implications
1452 for coldwater fishes. *Journal of Hydrology*, 588, 125066.
1453 <https://doi.org/10.1016/j.jhydrol.2020.125066>
- 1454 Letcher, B. H., Hocking, D. J., O’Neil, K., Whiteley, A. R., Nislow, K. H., & O’Donnell, M. J.
1455 (2016). A hierarchical model of daily stream temperature using air-water temperature
1456 synchronization, autocorrelation, and time lags. *PeerJ*, 4, e1727.
1457 <https://doi.org/10.7717/peerj.1727>
- 1458 Li, H., Deng, X., Kim, D.-Y., & Smith, E. P. (2014). Modeling maximum daily temperature
1459 using a varying coefficient regression model. *Water Resources Research*, 50(4), 3073–3087.
1460 <https://doi.org/10.1002/2013WR014243>
- 1461 ~~Liu, S., Xie, Z., Liu, B., Wang, Y., Gao, J., Zeng, Y., Xie, J., Xie, Z., Jia, B., Qin, P., Li, R.,~~
1462 ~~Wang, L., & Chen, S. (2020).~~ Global river water warming due to climate change and

- 1463 ~~anthropogenic heat emission. *Global and Planetary Change*, 193, 103289.~~
1464 ~~<https://doi.org/10.1016/j.gloplacha.2020.103289>~~
- 1465 Luce, C., Staab, B., Kramer, M., Wenger, S., Isaak, D., & McConnell, C. (2014). Sensitivity of
1466 summer stream temperatures to climate variability in the Pacific Northwest. *Water Resources*
1467 *Research*, 50(4), 3428–3443. <https://doi.org/10.1002/2013WR014329>
- 1468 Luo, Y., Ficklin, D. L., Liu, X., & Zhang, M. (2013). Assessment of climate change impacts on
1469 hydrology and water quality with a watershed modeling approach. *Science of The Total*
1470 *Environment*, 450–451, 72–82. <https://doi.org/10.1016/j.scitotenv.2013.02.004>
- 1471 ~~Lute, A. C., & Luce, C. H. (2017). Are model transferability and complexity antithetical?~~
1472 ~~*Insights from validation of a variable-complexity empirical snow model in space and time. *Water**~~
1473 ~~*Resources Research*, 53(11), 8825–8850. <https://doi.org/10.1002/2017WR020752>~~
- 1474 ~~Lusardi, R. A., Hammock, B. G., Jeffries, C. A., Dahlgren, R. A., & Kiernan, J. D. (2019).~~
1475 ~~*Oversummer growth and survival of juvenile coho salmon (*Oncorhynchus kisutch*) across a*~~
1476 ~~*natural gradient of stream water temperature and prey availability: An in situ enclosure*~~
1477 ~~*experiment. *Canadian Journal of Fisheries and Aquatic Sciences*, 1–12.*~~
1478 ~~<https://doi.org/10.1139/cjfas-2018-0484>~~
- 1479 Manhard, C. V., N. A. Som, E. C. Jones, & R. W. Perry. 2018. Estimation of stream conditions
1480 in tributaries of the Klamath River, Northern California (*Arcata Fisheries Technical Report*
1481 *Number TR 2018-32*). Arcata, CA: U.S. Fish and Wildlife Service.
1482 <https://web.archive.org/web/https://www.fws.gov/arcata/fisheries/reports/technical/2018/EstimationofStreamConditionsinTributariesoftheKlamathRiverNorthernCalifornia.pdf>
1483
- 1484 Mayer, T. D. (2012). Controls of summer stream temperature in the Pacific Northwest. *Journal*
1485 *of Hydrology*, 475(0), 323–335. <https://doi.org/10.1016/j.jhydrol.2012.10.012>
- 1486 ~~McGrath, E. O., Neumann, N. N., & Nichol, C. F. (2017). A statistical model for managing water~~
1487 ~~temperature in streams with anthropogenic influences. *River Research and Applications*, 33(1),~~
1488 ~~123–134. <https://doi.org/10.1002/rra.3057>~~
- 1489 Meier, W., Bonjour, C., Wüest, A., & Reichert, P. (2003). Modeling the effect of water diversion
1490 on the temperature of mountain streams. *Journal of Environmental Engineering*, 129(8), 755–
1491 764. [https://doi.org/10.1061/\(ASCE\)0733-9372\(2003\)129:8\(755\)](https://doi.org/10.1061/(ASCE)0733-9372(2003)129:8(755))
- 1492 ~~Menne, M. J., Durre, I., Korzeniewski, B., McNeal, S., Thomas, K., Yin, X., Anthony, S., Ray,~~
1493 ~~R., Vose, R. S., Gleason, B. E., & Houston, T. G. (2012a). Global historical climatology network~~
1494 ~~daily (GHCN Daily), version 3.26. NOAA National Climatic Data Center.~~
1495 ~~<http://doi.org/10.7289/V5D21VHZ>. Accessed 2021-01-11~~
- 1496 ~~Menne, M. J., Durre, I., Vose, R. S., Gleason, B. E., & Houston, T. G. (2012b). An overview of~~
1497 ~~the global historical climatology network daily database. *Journal of Atmospheric and Oceanic*~~
1498 ~~*Technology*, 29(7), 897–910. <https://doi.org/10.1175/JTECH-D-11-00103.1>~~
- 1499 Mierau, D. W., Trush, W. J., Rossi, G. J., Carah, J. K., Clifford, M. O., & Howard, J. K. (2017).
1500 Managing diversions in unregulated streams using a modified percent-of-flow approach.
1501 *Freshwater Biology*. <https://doi.org/10.1111/fwb.12985>

- 1502 Mohseni, O., & Stefan, H. G. (1999). Stream temperature/air temperature relationship: A
1503 physical interpretation. *Journal of Hydrology*, 218(3), 128–141. [https://doi.org/10.1016/S0022-](https://doi.org/10.1016/S0022-1694(99)00034-7)
1504 [1694\(99\)00034-7](https://doi.org/10.1016/S0022-1694(99)00034-7)
- 1505 Mohseni, O., Stefan, H. G., & Erickson, T. R. (1998). A nonlinear regression model for weekly
1506 stream temperatures. *Water Resources Research*, 34(10), 2685–2692.
1507 <https://doi.org/10.1029/98WR01877>
- 1508 Moore, R. D., Spittlehouse, D. L., & Story, A. (2005a, 2005). Riparian microclimate and
1509 stream temperature response to forest harvesting: A review. *Journal of the American Water*
1510 *Resources Association*, 41(4), 813–834. <https://doi.org/10.1111/j.1752-1688.2005.tb03772.x>
- 1511 Moore, R. D., Sutherland, P., Gomi, T., & Dhakal, A. (2005b). Thermal regime of a headwater
1512 stream within a clear-cut, coastal British Columbia, Canada. *Hydrological Processes*, 19(13),
1513 2591–2608. <https://doi.org/10.1002/hyp.5733>
- 1514 Moulton, T. L. (2018). *rMR: Importing Data from Loligo Systems Software, Calculating*
1515 *Metabolic Rates and Critical Tensions*. R package version 1.1.0. [https://CRAN.R-](https://CRAN.R-project.org/package=rMR)
1516 [project.org/package=rMR](https://CRAN.R-project.org/package=rMR)
- 1517 Muggeo, V. M. R., Sciadra, M., Tomasello, A., & Calvo, S. (2013). Estimating growth charts
1518 via nonparametric quantile regression: A practical framework with application in ecology.
1519 *Environmental and Ecological Statistics*, 20(4), 519–531. [https://doi.org/10.1007/s10651-](https://doi.org/10.1007/s10651-012-0232-1)
1520 [0232-1](https://doi.org/10.1007/s10651-012-0232-1)
- 1521 National Marine Fisheries Service (NMFS) (2014). *Final Recovery Plan for the Southern*
1522 *Oregon/Northern California Coast Evolutionarily Significant Unit of Coho Salmon*
1523 *(Oncorhynchus kisutch)*. Arcata, CA: National Marine Fisheries Service.
- 1524 Neumann David W., Rajagopalan Balaji, & Zagona Edith A. (2003). Regression model for daily
1525 maximum stream temperature. *Journal of Environmental Engineering*, 129(7), 667–674.
1526 [https://doi.org/10.1061/\(ASCE\)0733-9372\(2003\)129:7\(667\)](https://doi.org/10.1061/(ASCE)0733-9372(2003)129:7(667))
- 1527 Nichols, A. L., Willis, A. D., Jeffres, C. A., & Deas, M. L. (2014). Water temperature patterns
1528 below large groundwater springs: management implications for coho salmon in the Shasta River,
1529 California. *River Research and Applications*, 30(4), 442–455. <https://doi.org/10.1002/rra.2655>
- 1530 NCRWQCB (North Coast Regional Water Quality Control Board (NCRWQCB) (2005). *Staff*
1531 *Report for the Action Plan for the Scott River Watershed Sediment and Temperature Total*
1532 *Maximum Daily Loads*. Santa Rosa, CA: North Coast Regional Water Quality Control Board.
1533 https://www.waterboards.ca.gov/northcoast/water_issues/programs/tmdls/scott_river/staff_report
- 1534 Null, S. E., Mouzon, N. R., & Elmore, L. R. (2017). Dissolved oxygen, stream temperature, and
1535 fish habitat response to environmental water purchases. *Journal of Environmental Management*,
1536 197, 559–570. <https://doi.org/10.1016/j.jenvman.2017.04.016>
- 1537 Null, S. E., Viers, J. H., Deas, M. L., Tanaka, S. K., & Mount, J. F. (2013). Stream temperature
1538 sensitivity to climate warming in California's Sierra Nevada: Impacts to coldwater habitat.
1539 *Climatic Change*, 116(1), 149–170. <https://doi.org/10.1007/s10584-012-0459-8>
- 1540 Ouellet, V., St-Hilaire, A., Dugdale, S. J., Hannah, D. M., Krause, S., & Proulx-Ouellet, S.
1541 (2020). River temperature research and practice: Recent challenges and emerging opportunities

- 1542 for managing thermal habitat conditions in stream ecosystems. *Science of The Total*
1543 *Environment*, 736, 139679. <https://doi.org/10.1016/j.scitotenv.2020.139679>
- 1544 Pedersen, E. J., Miller, D. L., Simpson, G. L., & Ross, N. (2019). Hierarchical generalized
1545 additive models in ecology: An introduction with mgcv. *PeerJ*, 7, e6876.
1546 <https://doi.org/10.7717/peerj.6876>
- 1547 Persad, G. G., Swain, D. L., Kouba, C., & Ortiz-Partida, J. P. (2020). Inter-model agreement on
1548 projected shifts in California hydroclimate characteristics critical to water management. *Climatic*
1549 *Change*. <https://doi.org/10.1007/s10584-020-02882-4>
- 1550 ~~Pinheiro, J., Bates, D., DebRoy, S., Sarkar, D., & R Core Team (2020). *nlme: Linear and*
1551 *Nonlinear Mixed Effects Models*. R package version 3.1-148. [https://CRAN.R-](https://CRAN.R-project.org/package=nlme)
1552 [project.org/package=nlme](https://CRAN.R-project.org/package=nlme).~~
- 1553 Piotrowski, A. P., & Napiorkowski, J. J. (2019). Simple modifications of the nonlinear
1554 regression stream temperature model for daily data. *Journal of Hydrology*, 572, 308–328.
1555 <https://doi.org/10.1016/j.jhydrol.2019.02.035>
- 1556 Poff, N. L., Tharme, R. E., & Arthington, A. H. (2017). ~~Chapter 11—~~Evolution of environmental
1557 flows assessment science, principles, and methodologies. In A. C. Horne, J. A. Webb, M. J.
1558 Stewardson, B. Richter, & M. Acreman (Eds.), *Water for the Environment* (pp. 203–236).
1559 Academic Press. <https://doi.org/10.1016/B978-0-12-803907-6.00011-5>
- 1560 ~~Power, M. E., & Dietrich, W. E. (2002). Food webs in river networks. *Ecological Research*,~~
1561 ~~17(4), 451–471.~~
- 1562 ~~QVIR (Quartz Valley Indian Reservation-QVIR) (2016). Quality assurance project plan 2016~~
1563 ~~revision water quality sampling and analysis, CWA 106 grant identification # I-96927206-0. Fort~~
1564 ~~Jones, CA: QVIR Tribal Environmental Protection Department.~~
- 1565 ~~Railsback, S. F., Harvey, B. C., Kupferberg, S. J., Lang, M. M., McBain, S., & Welsh, H. H.~~
1566 ~~(2016). Modeling potential river management conflicts between frogs and salmonids. *Canadian*~~
1567 ~~*Journal of Fisheries and Aquatic Sciences*, 73(5), 773–784. [https://doi.org/10.1111/ecog.02881](https://doi.org/10.1139/cjfas-2015-
1568 0267</p><p>1569 Roberts, D. R., Bahn, V., Ciuti, S., Boyce, M. S., Quigley, D., Färber, S., Conner, Elith, J.,
1570 Guillera-Arroita, G., Hauenstein, S., Lahoz-Monfort, J. J., Schröder, B., Thuiller, W., Warton, D.
1571 I., Wintle, B. A., Hartig, F., & Dormann, C. F. (2017). Cross-validation strategies for data with
1572 temporal, spatial, hierarchical, or phylogenetic structure. <i>Ecography</i>, 40(8), 913–929.
1573 <a href=)~~
- 1574 ~~Romberger, C. Z. and S. Gwozdz (2018). Performance of water temperature management on the~~
1575 ~~Klamath and Trinity Rivers, 2017. (U.S. Fish and Wildlife Service, Arcata Fisheries Data Series~~
1576 ~~Number DS 2018-59).~~
- 1577 ~~K., Power, J., & Bundy, L. (2001). Water Temperatures in the Scott River Watershed in~~
1578 ~~Northern California. [https://web.archive.org/web/http://www.fws.gov/yreka/Final-](https://web.archive.org/web/http://www.fws.gov/yreka/Final-Reports/rmaap/2000-JTW-01-SRCD.pdf)~~
1579 ~~Reports/rmaap/2000-JTW-01-SRCD.pdf~~
- 1580 ~~R Core Team (2020). *R: A language and environment for statistical computing*. Vienna, Austria:~~
1581 ~~R Foundation for Statistical Computing. <https://www.R-project.org/>.~~

- 1582 [Rahmani, F., Lawson, K., Ouyang, W., Appling, A., Oliver, S., & Shen, C. \(2020\). Exploring the](#)
1583 [exceptional performance of a deep learning stream temperature model and the value of](#)
1584 [streamflow data. *Environmental Research Letters*. <https://doi.org/10.1088/1748-9326/abd501>](#)
- 1585 Santiago, J. M., Muñoz-Mas, R., Solana-Gutiérrez, J., García de Jalón, D., Alonso, C., Martínez-
1586 Capel, F., Pórtoles, J., Monjo, R., & Ribalaygua, J. (2017). Waning habitats due to climate
1587 change: The effects of changes in streamflow and temperature at the rear edge of the distribution
1588 of a cold-water fish. *Hydrology and Earth System Sciences*, 21(8), 4073–4101.
1589 <https://doi.org/10.5194/hess-21-4073-2017>
- 1590 [Segura, C., Caldwell, P., Sun, G., McNultyShaw, S., & Zhang, Y. \(2015\). A model. B. \(2017\).](#)
1591 [Does an upper limit to predict streamriver water temperature across the conterminous USA apply](#)
1592 [in all places? *Hydrological Processes*, 29\(9\), 2178–2195.31\(21\), 3729–3739.](#)
1593 <https://doi.org/10.1002/hyp.4035711297>
- 1594 Siegel, J. E., & Volk, C. J. (2019). Accurate spatiotemporal predictions of daily stream
1595 temperature from statistical models accounting for interactions between climate and landscape.
1596 *PeerJ*, 7, e7892. <https://doi.org/10.7717/peerj.7892>
- 1597 Sinokrot, B. A., & Gulliver, J. S. (2000). In-stream flow impact on river water temperatures.
1598 *Journal of Hydraulic Research*, 38(5), 339–349. <https://doi.org/10.1080/00221680009498315>
- 1599 Sohrabi, M. M., Benjankar, R., Tonina, D., Wenger, S. J., & Isaak, D. J. (2017). Estimation of
1600 daily stream water temperatures with a Bayesian regression approach. *Hydrological Processes*,
1601 31(9), 1719–1733. <https://doi.org/10.1002/hyp.11139>
- 1602 [Smith, C. D., Rounds, S. A., & Orzol, L. L. \(2018\). Klamath River Basin water-quality data.](#)
1603 [\(USGS Numbered Series *Fact Sheet* 2018–3031\). <https://doi.org/10.3133/fs20183031>](#)
- 1604 Soto, B. (2016). Assessment of Trends in Stream Temperatures in the North of the Iberian
1605 Peninsula Using a Nonlinear Regression Model for the Period 1950–2013. *River Research and*
1606 *Applications*, 32(6), 1355–1364. <https://doi.org/10.1002/rra.2971>
- 1607 Stanford, J.A. & Ward, J.V. (1992). Management of aquatic resources in large catchments:
1608 Recognizing interactions between ecosystem connectivity and environmental disturbance. In R.
1609 J. Naiman (Editor). *Watershed Management: Balancing Sustainability and Environmental*
1610 *Change* (pp. 91–124). New York, NY: Springer.
- 1611 St-Hilaire, A., Boyer, C., Bergeron, N., & Daigle, A. (2018). Water temperature monitoring in
1612 Eastern Canada: A case study for network optimization. *WIT Transactions on Ecology and the*
1613 *Environment*, 228, 269–275. <https://doi.org/10.2495/WP180251>
- 1614 [Steel, E. A., Beechie, T. J., Torgersen, C. E., & Fullerton, A. H. \(2017\). Envisioning,](#)
1615 [quantifying, and managing thermal regimes on river networks. *BioScience*, 67\(6\), 506–522.](#)
1616 <https://doi.org/10.1093/biosci/bix047>
- 1617 ~~Kennedy, M. C., Cunningham, P. G., & Stanovick, J. S. (2013). Applied statistics in ecology:~~
1618 ~~Common pitfalls and simple solutions. *Ecosphere*, 4(9), art115. [https://doi.org/10.1890/ES13-](https://doi.org/10.1890/ES13-00160.1)~~
1619 ~~00160.1~~
- 1620 [Steel, E. A., Tillotson, A., Larsen, D. A., Fullerton, A. H., Denton, K. P., & Beekman, B. R.](#)
1621 [\(2012\). Beyond the mean: The role of variability in predicting ecological effects of stream](#)
1622 [temperature on salmon. *Ecosphere*, 3\(11\), 1–11. <https://doi.org/10.1890/ES12-00255.1>](#)

- 1623 [Stenhouse, S., Pisano, M., Bean, C., & Chesney, W. \(2012\). Water temperature thresholds for](#)
1624 [coho salmon in a spring-fed river, Siskiyou County, California. *California Fish and Game*, 98\(1\),](#)
1625 [19–27.](#)
- 1626 Superior Court of Siskiyou County (1980). Scott River adjudication, decree no. 30662. Scott
1627 River stream system, Siskiyou County. Sacramento, CA: State Water Resources Control Board.
- 1628 Sutton, R. J., Deas, M. L., Tanaka, S. K., Soto, T., & Corum, R. A. (2007). Salmonid
1629 observations at a Klamath River thermal refuge under various hydrological and meteorological
1630 conditions. *River Research and Applications*, 23(7), 775–785.
- 1631 Sutton, R., & Soto, T. (2012). Juvenile coho salmon behavioural characteristics in Klamath river
1632 summer thermal refugia. *River Research and Applications*. <https://doi.org/10.1002/rra.1459>
- 1633 [Tan, J., & Cherkauer, K. A. \(2013\). Assessing Tague, C., Farrell, M., Grant, G., Lewis, S., &](#)
1634 [Rey, S. \(2007\). Hydrogeologic controls on summer stream temperature variation temperatures in](#)
1635 [the Pacific Northwest using airborne thermal infrared remote sensing. *Journal of Environmental*](#)
1636 [Management](#), 115, 206–216. McKenzie River basin, Oregon. *Hydrological Processes*, 21(24),
1637 [3288–3300. <https://doi.org/10.1016/j.jenvman.2012.10.042>](#)
[1002/hyp.6538](#)
- 1638 [Toffolon, M., & Piccolroaz, S. \(2015\). A hybrid model for river water temperature as a function](#)
1639 [of air temperature and discharge. *Environmental Research Letters*, 10\(11\), 114011.](#)
1640 <https://doi.org/10.1088/1748-9326/10/11/114011>
- 1641 [Theurer, F.D., Voos, K.A., & Miller, W.J. \(1984\). Instream water temperature model. *Instream*](#)
1642 [Flow Information Paper 16. FWS/OBS-84/15. Washington, D.C.: US Fish and Wildlife Service.](#)
- 1643 Tolley, D., Foglia, L., & Harter, T. (2019). Sensitivity analysis and calibration of an integrated
1644 hydrologic model in an irrigated agricultural basin with a groundwater-dependent ecosystem.
1645 *Water Resources Research*, 55(9), 7876–7901. <https://doi.org/10.1029/2018WR024209>
- 1646 [USEPA \(U.S. Environmental Protection Agency\) \(2003\). EPA Region 10 guidance for Pacific](#)
1647 [Northwest state and tribal temperature water quality standards. EPA 910-B-03-002. Seattle, WA:](#)
1648 [Region 10 Office of Water.](#)
- 1649 Van Kirk, R. W., & Naman, S. W. (2008). Relative effects of climate and water use on base-flow
1650 trends in the Lower Klamath Basin. *Journal of the American Water Resources Association*,
1651 44(4), 1035–1052. <https://doi.org/10.1111/j.1752-1688.2008.00212.x>
- 1652 [VanderKooi, S., Thorsteinson, L., & Clark, M. \(2011\). Environmental and historical setting. In](#)
1653 [L. Thorsteinson, S. VanderKooi, & W. Duffy \(Eds.\), *Proceedings of the Klamath Basin Science*](#)
1654 [Conference, Medford, Oregon, February 1–5, 2010 \(pp. 31–36\). Reston, VA: U.S. Geological](#)
1655 [Survey.](#)
- 1656 van Rij, J., Hendriks, P., van Rijn, H., Baayen, R. H., & Wood, S. N. (2019). Analyzing the time
1657 course of pupillometric data. *Trends in Hearing*, 23, 233121651983248.
1658 <https://doi.org/10.1177/2331216519832483>
- 1659 van Rij, J., Wieling, M., Baayen, R., van Rijn, H. (2020). itsadug: Interpreting time series and
1660 autocorrelated data using GAMMs. *R package version 2.4*. [https://cran.r-](https://cran.r-project.org/package=itsadug)
1661 [project.org/package=itsadug](https://cran.r-project.org/package=itsadug)

- 1662 van Vliet, M. T. H., Ludwig, F., Zwolsman, J. J. G., Weedon, G. P., & Kabat, P. (2011). Global
1663 river temperatures and sensitivity to atmospheric warming and changes in river flow. *Water*
1664 *Resources Research*, 47(2). <https://doi.org/10.1029/2010WR009198>
- ~~1665 Wanders, N., Vliet, M. T. H. van, Wada, Y., Bierkens, M. F. P., & Beek, L. P. H. (Rens) van.~~
~~1666 (2019). High Resolution Global Water Temperature Modeling. *Water Resources Research*,~~
~~1667 *55*(4), 2760–2778. <https://doi.org/10.1029/2018WR023250>~~
- 1668 Webb, B. W., Clack, P. D., & Walling, D. E. (2003). Water–air temperature relationships in a
1669 Devon river system and the role of flow. *Hydrological Processes*, 17(15), 3069–3084.
1670 <https://doi.org/10.1002/hyp.1280>
- 1671 Webb, B. W., Hannah, D. M., Moore, R. D., Brown, L. E., & Nobilis, F. (2008). Recent
1672 advances in stream and river temperature research. *Hydrological Processes*, 22(7), 902–918.
1673 <https://doi.org/10.1002/hyp.6994>
- ~~1674 Webb, B. W., & Walling, D. E. (1993). Temporal variability in the impact of river regulation on~~
~~1675 *thermal regime and some biological implications. *Freshwater Biology*, 29(1), 167–182.*~~
~~1676 <https://doi.org/10.1111/j.1365-2427.1993.tb00752.x>~~
- ~~1677 Welch, H. H., Hodgson, G. R., Harvey, B. C., & Roche, M. F. (2001). Distribution of juvenile~~
~~1678 *coho salmon in relation to water temperatures in tributaries of the Mattole River, California.*~~
~~1679 *North American Journal of Fisheries Management*, 21(3), 464–470.~~
~~1680 [https://doi.org/10.1577/1548-8675\(2001\)021<0464:DOJCSI>2.0.CO;2](https://doi.org/10.1577/1548-8675(2001)021<0464:DOJCSI>2.0.CO;2)~~
- 1681 Wenger, S. J., Isaak, D. J., Luce, C. H., Neville, H. M., Fausch, K. D., Dunham, J. B., Dauwalter,
1682 D. C., Young, M. K., Elsner, M. M., Rieman, B. E., Hamlet, A. F., & Williams, J. E. (2011).
1683 Flow regime, temperature, and biotic interactions drive differential declines of trout species
1684 under climate change. *Proceedings of the National Academy of Sciences*, 108(34), 14175–14180.
1685 <https://doi.org/10.1073/pnas.1103097108>
- ~~1686 Wondzell, S. M., Diabat, M., & Haggerty, R. (2019). What Matters Most: Are Future Stream~~
~~1687 *Temperatures More Sensitive to Changing Air Temperatures, Discharge, or Riparian Vegetation?*~~
~~1688 *Journal of the American Water Resources Association*, 55(1), 116–132.~~
~~1689 <https://doi.org/10.1111/1752-1688.12707>~~
- 1690 Westerling, A. L. (2016). Increasing western US forest wildfire activity: Sensitivity to changes in
1691 the timing of spring. *Philosophical Transactions of the Royal Society B: Biological Sciences*,
1692 371(1696), 20150178. <https://doi.org/10.1098/rstb.2015.0178>
- 1693 Wood, S.N. (2017). *Generalized additive models: An introduction with R (2nd edition)*.
1694 Chapman and Hall/CRC.
- 1695 Wrzesiński, D., & Graf, R. (2022). Temporal and spatial patterns of the river flow and water
1696 temperature relations in Poland. *Journal of Hydrology and Hydromechanics*, 70(1), 12–29.
1697 <https://doi.org/10.2478/johh-2021-0033>
- 1698 Yan, H., Sun, N., Fullerton, A., & Baerwalde, M. (2021). Greater vulnerability of snowmelt-fed
1699 river thermal regimes to a warming climate. *Environmental Research Letters*, 16(5), 054006.
1700 <https://doi.org/10.1088/1748-9326/abf393>

- 1701 Yang, G., & Moyer, D. L. (2020). Estimation of nonlinear water-quality trends in high-frequency
1702 monitoring data. *Science of The Total Environment*, 715, 136686.
1703 <https://doi.org/10.1016/j.scitotenv.2020.136686>
- 1704 Yard, M. D., Bennett, G. E., Mietz, S. N., Coggins, L. G., Stevens, L. E., Hueftle, S., & Blinn, D.
1705 W. (2005). Influence of topographic complexity on solar insolation estimates for the Colorado
1706 River, Grand Canyon, AZ. *Ecological Modelling*, 183(2), 157–172.
1707 <https://doi.org/10.1016/j.ecolmodel.2004.07.027>
- 1708 Yarnell, S. M., Stein, E. D., Webb, J. A., Grantham, T., Lusardi, R. A., Zimmerman, J., Peck, R.
1709 A., Lane, B. A., Howard, J., & Sandoval-Solis, S. (2020). A functional flows approach to
1710 selecting ecologically relevant flow metrics for environmental flow applications. *River Research
1711 and Applications*, rra.3575. <https://doi.org/10.1002/rra.3575>

1712

1713 **References From the Supporting Information**

- 1714 [Daly, C., Doggett, M. K., Zhu, S., Heddam, S., Nyarko, E. K., Hadzima-Nyarko, M., Piccolroaz,](#)
1715 [S., & Wu, S. \(2018\). Modeling daily water temperature for rivers: Comparison between adaptive](#)
1716 [neuro-fuzzy inference systems and artificial neural networks models. *Environmental Science and*](#)
1717 [Pollution Research](#). <https://doi.org/10.1007/s11356-018-3650-2>
- 1718 [Zhu, S., & Piotrowski, A. P. \(2020\). River/stream water temperature forecasting using artificial](#)
1719 [intelligence models: A systematic review. *Acta Geophysica*, 68\(5\), 1433–1442.](#)
1720 <https://doi.org/10.1007/s11600-020-00480-7>
- 1721 [Smith, J. I., Olson, K. V., Halbleib, M. D., Dimcovic, Z., Keon, D., Loiselle, R. A., Steinberg,](#)
1722 [B., Ryan, A. D., Pancake, C. M., & Kaspar, E. M. \(2021\). Challenges in observation-based](#)
1723 [mapping of daily precipitation across the conterminous United States. *Journal of Atmospheric*](#)
1724 [and Oceanic Technology](#), 38(11), 1979–1992. <https://doi.org/10.1175/JTECH-D-21-0054.1>
- 1725 [Lusardi, R. A., Hammock, B. G., Jeffres, C. A., Dahlgren, R. A., & Kiernan, J. D. \(2019\).](#)
1726 [Oversummer growth and survival of juvenile coho salmon \(*Oncorhynchus kisutch*\) across a](#)
1727 [natural gradient of stream water temperature and prey availability: An in situ enclosure](#)
1728 [experiment. *Canadian Journal of Fisheries and Aquatic Sciences*, 1–12.](#)
1729 <https://doi.org/10.1139/cjfas-2018-0484>
- 1730 [McGrath, E. O., Neumann, N. N., & Nichol, C. F. \(2017\). A statistical model for managing water](#)
1731 [temperature in streams with anthropogenic influences. *River Research and Applications*, 33\(1\),](#)
1732 [123–134. <https://doi.org/10.1002/rra.3057>](#)
- 1733 [Menne, M.J., Durre, I., Korzeniewski, B., McNeal, S., Thomas, K., Yin, X., Anthony, S., Ray,](#)
1734 [R., Vose, R.S., Gleason, B.E., & Houston, T.G. \(2012a\). Global historical climatology network -](#)
1735 [daily \(GHCN-Daily\), version 3.26. NOAA National Climatic Data Center.](#)
1736 <http://doi.org/10.7289/V5D21VHZ>. Accessed 2021-01-11
- 1737 [Menne, M. J., Durre, I., Vose, R. S., Gleason, B. E., & Houston, T. G. \(2012b\). An overview of](#)
1738 [the global historical climatology network-daily database. *Journal of Atmospheric and Oceanic*](#)
1739 [Technology](#), 29(7), 897–910. <https://doi.org/10.1175/JTECH-D-11-00103.1>

- 740 [Moore, R. B., & Dewald, T. G. \(2016\). The road to NHDPlus—Advancements in digital stream](#)
741 [networks and associated catchments. *Journal of the American Water Resources Association*,](#)
742 [52\(4\), 890–900. https://doi.org/10.1111/1752-1688.12389](#)
- 743 [Steel, E. A., Kennedy, M. C., Cunningham, P. G., & Stanovick, J. S. \(2013\). Applied statistics in](#)
744 [ecology: Common pitfalls and simple solutions. *Ecosphere*, 4\(9\), art115.](#)
745 [https://doi.org/10.1890/ES13-00160.1](#)
- 746 [Stenhouse, S., Pisano, M., Bean, C., & Chesney, W. \(2012\). Water temperature thresholds for](#)
747 [coho salmon in a spring fed river, Siskiyou County, California. *California Fish and Game*, 98\(1\),](#)
748 [19–37.](#)
- 749 [Welsh, H. H., Hodgson, G. R., Harvey, B. C., & Roche, M. F. \(2001\). Distribution of juvenile](#)
750 [coho salmon in relation to water temperatures in tributaries of the Mattole River, California.](#)
751 [*North American Journal of Fisheries Management*, 21\(3\), 464–470.](#)
752 [https://doi.org/10.1577/1548-8675\(2001\)021<0464:DOJCSI>2.0.CO;2](#)
- 1753 Zillig, K. W., Lusardi, R. A., Moyle, P. B., & Fangue, N. A. (2021). One size does not fit all:
1754 Variation in thermal eco-physiology among Pacific salmonids. *Reviews in Fish Biology and*
1755 *Fisheries*. [https://doi.org/10.1007/s11160-020-09632-w](#)